



HAL
open science

Tailor-made microbial consortium for Kombucha fermentation: Microbiota-induced biochemical changes and biofilm formation

Océane Savary, Jérôme Mounier, Anne Thierry, Elisabeth Poirier, Julie Jourdren, Marie-Bernadette Maillard, Marine Penland, Christophe Decamps, Emmanuel Coton, Monika Coton

► To cite this version:

Océane Savary, Jérôme Mounier, Anne Thierry, Elisabeth Poirier, Julie Jourdren, et al.. Tailor-made microbial consortium for Kombucha fermentation: Microbiota-induced biochemical changes and biofilm formation. *Food Research International*, 2021, 147, pp.110549. 10.1016/j.foodres.2021.110549 . hal-03279810v1

HAL Id: hal-03279810

<https://hal.inrae.fr/hal-03279810v1>

Submitted on 7 Jul 2021 (v1), last revised 13 Oct 2023 (v2)

HAL is a multi-disciplinary open access archive for the deposit and dissemination of scientific research documents, whether they are published or not. The documents may come from teaching and research institutions in France or abroad, or from public or private research centers.

L'archive ouverte pluridisciplinaire **HAL**, est destinée au dépôt et à la diffusion de documents scientifiques de niveau recherche, publiés ou non, émanant des établissements d'enseignement et de recherche français ou étrangers, des laboratoires publics ou privés.



Distributed under a Creative Commons Attribution - NonCommercial - NoDerivatives 4.0 International License



Tailor-made microbial consortium for Kombucha fermentation: Microbiota-induced biochemical changes and biofilm formation

Océane Savary^a, Jérôme Mounier^a, Anne Thierry^b, Elisabeth Poirier^a, Julie Jourden^{a,c}, Marie-Bernadette Maillard^b, Marine Penland^a, Christophe Decamps^c, Emmanuel Coton^a, Monika Coton^{a,*}

^a Univ Brest, Laboratoire Universitaire de Biodiversité et Écologie Microbienne, F-29280 Plouzané, France

^b INRAE, Institut Agro, STLO, F-3500 Rennes, France

^c Biogroupe, 11 rue Robert Surcouf, 22430 Erquy, France

ARTICLE INFO

Keywords:

Kombucha
Fermentation dynamics
Metagenetics
Biochemical changes
Biofilm
Confocal microscopy
SEM

ABSTRACT

Kombucha is a very distinct naturally fermented sweetened tea that has been produced for thousands of years. Fermentation relies on metabolic activities of the complex autochthonous symbiotic microbiota embedded in a floating biofilm and used as a backstop for successive fermentations. Here, we designed a tailor-made microbial consortium representative of the core Kombucha microbiota to drive this fermentation. Microbial (counts, metagenetics), physico-chemical (pH, density) and biochemical (organic acids, volatile compounds) parameters were monitored as well as biofilm formation by confocal laser scanning microscopy and scanning electron microscopy. While nine species were co-inoculated, four (*Dekkera bruxellensis*, *Hanseniaspora uvarum*, *Acetobacter okinawensis* and *Liquorilactobacillus nagelii*) largely dominated. Microbial activities led to acetic, lactic, succinic and oxalic acids being produced right from the start of fermentation while gluconic and glucuronic acids progressively increased. A distinct shift in volatile profile was also observed with mainly aldehydes identified early on, then high abundances of fatty acids, ketones and esters at the end. Correlation analyses, combining metabolomic and microbial data also showed a shift in species abundances during fermentation. We also determined distinct bacteria-yeast co-occurrence patterns in biofilms by microscopy. Our study provides clear evidence that a tailor-made consortium can be successfully used to drive Kombucha fermentations.

1. Introduction

For centuries, humans have relied on fermentations to preserve foods and beverages but also to diversify products with specific organoleptic, nutritional and health properties. The microbial ecology of many well-known fermented products (i.e. wine, beer, cheese, dry cured meats, olives, sourdough...) has been widely studied by the scientific community to unravel the complex microbial communities involved in fermentation, determine co-occurrence patterns and, in some cases, the roles of the key fermentation drivers (Bokulich et al., 2016; Bourdichon et al., 2012; Coton et al., 2017; Fremaux et al., submitted; Landis et al., 2021; Liu, Zhang, Chen, & Howell, 2019; Montel et al., 2014; Mounier et al., 2005; Penland et al., 2020; Spitaels et al., 2015; Tyakht et al., 2021; Yeluri Jonnala, McSweeney, Sheehan, & Cotter, 2018). For naturally fermented products, solely relying on autochthonous

microorganisms for fermentation, these studies are of particular interest as it may lead to novel starter selection and fermentation drivers with specific and desirable traits for a given product.

Kombucha is a naturally fermented effervescent beverage with a slightly acidic, refreshing and distinct taste originating from North-eastern China, about 220 B.C (Jayabalan, Malbaša, Lončar, Vitas, & Sathishkumar, 2014). It is globally distributed and has become increasingly popular in North America and Europe (Coton et al., 2017) due to strong consumer demands for more natural and healthier products that keep their signature characteristics. Kombucha is prepared using sweetened black or green teas and fermented by symbiotic cultures of autochthonous yeasts, acetic acid bacteria (AAB) and lactic acid bacteria (LAB) embedded in a floating biofilm for, on average, 8 to 15 days under aerobic and static conditions (Coton et al., 2017) although longer fermentations (~1 month) may occur. The microbially rich

* Corresponding author.

E-mail address: monika.coton@univ-brest.fr (M. Coton).

<https://doi.org/10.1016/j.foodres.2021.110549>

Received 15 March 2021; Received in revised form 28 May 2021; Accepted 16 June 2021

Available online 18 June 2021

0963-9969/© 2021 Elsevier Ltd. All rights reserved.

Kombucha biofilm is successively used as a starter, or backslap, for future fermentations and often shared between producers worldwide. Microbial compositions of many Kombuchas has been recently studied using both metagenetics and metagenomics sequencing approaches (Arkan, Mitchell, Finn, & Gürel, 2020; Chakravorty et al., 2016; Coton et al., 2017; De Filippis, Troise, Vitaglione, & Ercolini, 2018; Gaggia et al., 2019; Marsh, O'Sullivan, Hill, Ross, & Cotter, 2014; Reva et al., 2015; Villarreal-Soto et al., 2020) and, in some cases, linked to culture-dependent techniques (Coton et al., 2017). This is particularly of interest to determine species co-occurrence patterns but also to access, preserve and exploit the identified microbial diversity via culturing techniques. These studies, regardless of geographical origin, have all highlighted the widespread presence of certain fungal and bacterial species interacting through highly symbiotic relationships and cooperative metabolism. Among yeasts, *Dekkera* spp. (e.g. *D. anomala*, *D. bruxellensis*), *Pichia* spp. (e.g. *P. occidentalis*), *Yarrowia* spp. (e.g. *Y. lipolytica*), *Candida* spp. (e.g. *C. zemplinina*), *Saccharomycetales* spp., *Hanseniaspora* spp. (e.g. *H. valbyensis*) and *Zygosaccharomyces* spp. (e.g. *Z. bailii*) were among the most dominant and prevalent species (Arkan et al., 2020; Chakravorty et al., 2016; Chen & Liu, 2000; Coton et al., 2017; De Filippis et al., 2018; Gaggia et al., 2019; Hesseltine, 1965; Jankovic & Stojanovic, 1994; Jayabalan et al., 2014; Liu, Hsu, Lee, & Liao, 1996; S. L. Markov et al., 2001; Marsh et al., 2014; Maysner, Fromme, Leitzmann, & Gründer, 1995; Reva et al., 2015; Teoh, Heard, & Cox, 2004; Villarreal-Soto et al., 2020), although not all species are systematically identified thus not necessarily part of the Kombucha core microbiota. Among bacteria, *Proteobacteria* phylum is systematically observed with a strong prevalence of AAB. The most frequent genera and species include *Komagataeibacter* (formerly *Gluconacetobacter*) (e.g. *K. xylinus*, *K. europaeus*, *K. rhaeticus*), *Gluconobacter* (e.g. *G. oxydans*) and sometimes *Acetobacter* (e.g. *A. tropicalis*, *A. okinawensis*) (Arkan et al., 2020; Chakravorty et al., 2016; Coton et al., 2017; De Filippis et al., 2018; Gaggia et al., 2019; Greenwalt, Steinkraus, & Ledford, 2000; Jankovic & Stojanovic, 1994; Jayabalan, Malini, Sathishkumar, Swaminathan, & Yun, 2010; Kurtzman, Robnett, & Basehoar-Powers, 2001; Liu et al., 1996; Marsh et al., 2014; Reva et al., 2015; Villarreal-Soto et al., 2020). Some studies have also highlighted LAB, although less abundant than AAB with *Lactobacillus* spp. (e.g. *Liquorilactobacillus nagelii*), *Oenococcus oeni* and/or *Bifidobacterium* being identified (Coton et al., 2017; Teoh et al., 2004). These microorganisms co-occur in the tea fraction and/or are embedded in the floating cellulosic biofilm regenerated with each new fermentation, also named “mother”, “tea fungus” or “SCOBY”, for “Symbiotic Community of Bacteria and Yeast” (Jayabalan et al., 2014; May et al., 2019; Villarreal-Soto et al., 2018). The stability and maintenance of the biofilm microbiome over time has yet to be characterized despite its intense use as a backslap for fermentations. During fermentation, this microbially rich biofilm floats on the surface of open fermentation tanks thus creating favorable aerobic conditions at the liquid–air interface for microbial interactions and cooperative metabolism. Indeed, yeasts break down the main carbon source, sucrose, initially added to the tea into glucose and fructose, and ferment them into two major end products, ethanol and CO₂ (Coton et al., 2017; Jayabalan et al., 2014; Villarreal-Soto et al., 2018). Then, bacteria, mainly AAB embedded in the biofilm, successively oxidize ethanol into acetic acid but also use glucose to produce other organic acids as acetic, succinic, gluconic or glucuronic acids (Arkan et al., 2020; Coton et al., 2017; Gomes, Borges, Rosa, Castro-Gómez, & Spinosa, 2018; Siniša L. Markov et al., 2003; Ramachandran, Fontanille, Pandey, & Larroche, 2006). These metabolites all contribute to the slightly acidic and sour taste of the final product but may also contribute to the potential health benefits associated with this product although further studies are needed. Some AAB species also play another key role during Kombucha fermentation as they can produce the cellulosic biofilm from simple sugars (Coton et al., 2017; Villarreal-Soto et al., 2018). LAB, although not systematically found, also produce organic acids and impact product acidity and the overall sensorial attributes. Overall, bacterial metabolic activities not only rapidly reduce

pH to values close to 3, but also decrease the ethanol produced by fermentative yeasts to values below 1.2%, which is in accordance with the designation “without alcohol” from the European regulation (EU N° 1169/2011).

Changes in biochemical profile during fermentation are related to the Kombucha microbiota and/or biofilm origins but also fermentation conditions, in particular vessel size, oxygen availability, temperature and tea type (Cardoso et al., 2020; Coton et al., 2017; Gaggia et al., 2019; Marsh et al., 2014). A full understanding of the role of this complex microbiota, whether embedded or not in a biofilm, during fermentation is thus needed to better maintain and control production conditions. In this sense, strain selection and associations for directed Kombucha fermentations is of clear interest as recently documented (S. Wang et al., 2020).

The goal of our study was to i) design a tailor-made microbial consortium by selecting the main microbial drivers from a previously described Kombucha core microbiota (Coton et al., 2017) to drive this fermentation and ii) determine its impact on fermentation by dynamically monitoring microbial populations (by enumerations and metagenetics), physico-chemical properties (pH and density), biochemical parameters (organic acids and volatile compounds), and biofilm formation using fluorescent *in situ* hybridization with microbial group specific probes coupled to confocal laser scanning microscopy and scanning electron microscopy analyses.

2. Materials and methods

2.1. Defined complex consortium for Kombucha fermentations

2.1.1. Consortium and culture conditions

The defined consortium included five ABB strains belonging to four species: *Acetobacter tropicalis* J2-MRN2-BA1.1, *A. okinawensis* J2-BSN3-BA4.1 and J0-MRN1-BA3.1, *Komagataeibacter hansenii* (formerly *Gluconacetobacter hansenii*) J0-MRC3-BA5.2 and *Gluconobacter oxydans* J0-BSD1-BA3.1, two LAB species: *Liquorilactobacillus nagelii* J0-BSV3-BL5 and *Oenococcus oeni* UBOCC-A-315005 and four yeast strains belonging to three species: *D. bruxellensis* J9-MRB2-Lev3.1 and J4-MRN1-Lev2.1, *Hanseniaspora uvarum* J9-MRD1-Lev2.2 and *Z. bailii* J9-BSB2-Lev5.3. All strains were previously isolated from black or green tea Kombucha fermentations (Coton et al., 2017). Cultures were directly prepared from cryo-conserved glycerol stocks at –80 °C by plating on appropriate media. Yeast extract glucose chloramphenicol agar (YGC, bioMérieux, France) was used for yeast cultures (incubation at 25 °C for 3–4 days) while AAB were plated on mannitol medium (D-mannitol 25 g/L, yeast extract 5 g/L, universal peptone 3 g/L and agar 15 g/L) supplemented with 0.1 g/L pimarinic acid and incubated at 30 °C for 3–4 days and LAB on De Man Rosaga Sharpe (MRS, bioMérieux, France) acidified with 10% (v/v) citric acid to pH 4.8 and supplemented with 0.1 g/L pimarinic acid and incubated at 30 °C for 3–4 days. Only MRS plates were incubated under anaerobic conditions in closed jars.

To calibrate cultures (between 10⁷ to 10⁸ colony-forming units (CFU)/mL), one colony was resuspended in 10 mL of broth and incubated for 72 h at 25 °C (yeast) or 30 °C (AAB, LAB). Yeast strains were cultivated in tryptic soy broth (bioMérieux, France) supplemented with 2.5 g/L yeast extract while AAB strains were cultivated in mannitol broth (D-mannitol 25 g/L, yeast extract 5 g/L, universal peptone 3 g/L) and LAB in MRS broth (bioMérieux, France). Then, a second culture was performed using a 1% inoculum in 10 mL broth and incubated for 24 h using the same conditions, except for *O. oeni* and *K. hansenii* that were incubated for 48 h. Yeast and AAB cultures were agitated at 120 rpm at 25 °C or 30 °C, respectively, while LAB were incubated at 30 °C under static conditions. All pure cultures were enumerated before inoculation to ensure target values of 10⁵ CFU/mL were obtained for fermentations.

2.1.2. Fermentation conditions

For fermentations, the consortium was then prepared by inoculating

each strain at a final concentration of 10^5 CFU/mL in 400 mL sweetened green tea. This was prepared by infusing dried tea leaves (placed in a paper filter) for 30 min in boiled distilled water supplemented with 55 g/L organic blond sugar and sterilized at 104 °C for 30 min. After homogenization, 800 mL lab scale fermentation vessels were covered with a sterilized linen sheet to create aerobic conditions and incubated at 25 °C for up to 27 days. Fermentation time was purposely extended to 27 days for biofilm formation and microscopy observations. For the dynamic follow-up, 16 biological replicates were performed and sampling was done at days 7, 11, 14, 20 and 27. An unfermented tea control sample was also included at day 0. For each date, 3 replicates were analyzed and the biofilm was recovered separately. The only exception was at d0, as no biofilm was yet formed.

2.2. Dynamic follow-up

2.2.1. Physico-chemical analyses

The indicators used to follow fermentation (pH, density and biofilm wet mass) were measured at each sampling day using 3 biological replicates. pH was determined using an electronic pH meter (Eutech Instruments, The Netherlands) and tea density was measured with a $1.000\text{--}1.100 \pm 0.001$ g/mL range densitometer at 20 °C (Fisher Scientific, France). Density measurements were specifically performed as a simple means to monitor sugar consumption during fermentation. Biofilm wet mass was measured using sterile conditions in Petri dishes and samples were kept for further analyses.

2.2.2. Microbiota monitoring

2.2.2.1. Microbial enumerations. AAB, LAB and yeast enumerations were carried out on both biofilm and Kombucha tea samples. For tea samples, serial dilutions were performed with tryptone salt (TS, Merck) while for biofilms, 1 g was transferred into 50 mL tubes containing 9 mL TS and homogenized with a sterile Ultra-Turrax^R (IKA, Germany) before being placed in a sterile stomacher bag equipped with a filter membrane and mixed for 180 s using a Stomacher (AES, France). The liquid fraction was collected and 1 mL was used for serial dilutions in TS while the remaining aliquot was conserved for downstream analyses. For both tea and biofilm aliquots, dilutions were plated on YGC for yeast, mannitol for AAB and MRS for LAB counts using an automatic spiral plater method (Interscience, France). Petri dishes were incubated using the same conditions as described above.

2.2.2.2. Metabarcoding. For total DNA extractions from tea samples, 15 mL were collected and centrifuged at 6654 g for 5 min at 4 °C. Supernatants were collected, filtered using 0.45 µm PTFE filters (Sartorius) and kept at -20 °C until further analyses by LC-MS while cells pellets were stored at -20 °C for DNA extractions. For biofilm samples, 4 mL of the homogenate prepared for microbial enumerations were collected and centrifuged using the same conditions and cell pellets were stored at -20 °C for DNA extractions.

DNA extractions were performed using an optimized version of the protocol described by Coton et al. (2017). This included an additional cell lysis step by adding 300 mg glass beads (<212 µm) to cells after incubation with the lysis buffer. Cells were then lysed using a vibro-crusher (Grosseron, France) twice for 30 s at 30 Hz and kept on ice for 5 min between each step before continuing the protocol as previously described. DNA extracts were quantified using a Nanodrop 1000 Spectrophotometer (ThermoFischer Scientific, USA) and adjusted to 20 ng/µL for downstream MiSeq PE300 sequencing at the Genome Quebec sequencing platform (McGill University, Canada). PCRs were performed by targeting the V3-V4 region of the bacterial 16S rRNA gene using the S-D-bact-0341-b-S-17 (5'-CCTACGGGNGGCWGCAG-3') and S-D-Bact-0785-a-A-21 (5'-GACTACHVGGGTATCTAATCC-3') primers (Klindworth et al., 2013), and the 26S yeast rDNA D1/D2 region using the NL1

5'-GCATATCAATAAGCGGAGGAAAAG-3' and NL4 5'-GGTCCGTGTTTCAAGACGG-3' primers (O'Donnell, 1993). This technology generated 2x300 bp reads and a total of 3.3 Gb of data for both amplicon types derived from the 31 samples.

2.2.2.3. Bioinformatics and data analyses. The DADA2 library (Callahan et al., 2016) was used in R version 3.5.0 (R Core Team, 2019) for 16S and 26S rRNA gene reads filtering. For 16S and 26S analyzes, 2 698 218 reads and 2 650 330 reads respectively were conserved with a normalization on the smallest number of reads found in a sample, 15 301 and 64 750 respectively. For 16S rRNA gene reads, forward and reverse read pairs were trimmed and filtered, with forward reads truncated at 270 bp and reverse reads at 210 bp, no ambiguous bases allowed and each read required to have less than two expected errors based on their quality scores. Amplicon sequence variants (ASVs) were independently inferred from the forward and reverse reads of each sample using the run-specific error rates, and then read pairs were merged requiring at least 15 bp overlap. For 26S rDNA reads, only forward reads were trimmed and filtered, with truncation at 300 bp, no ambiguous bases allowed and each read required to have less than two expected errors based on their quality scores. ASVs were directly inferred from forward reads.

16S chimera sequences were removed using UCHIME algorithm (Edgar, Haas, Clemente, Quince, & Knight, 2011) implemented in VSEARCH v1.1.3 (<https://github.com/torognes/vsearch>) against the ChimeraS-layer reference database (Haas et al., 2011) and the RDP classifier (Q. Wang, Garrity, Tiedje, & Cole, 2007) was used for taxonomy assignment, which was made with GreenGenes v13.8 database (McDonald et al., 2012) available in Qiime (Caporaso et al., 2010). Each 16S ASV was then classified to the species level using the RDP seqmatch tool (<https://rdp.cme.msu.edu/seqmatch>). 26S rRNA gene ASVs were assigned to the species level using the BLAST algorithm (<http://www.ncbi.nlm.nih.gov/BLAST/>).

Beta diversity analyses based on Bray-Curtis distances were performed using the Calypso software tool v8.84 (Zakrzewski et al., 2017) after total sum normalization of count data combined with square root transformation (Hellinger transformation).

2.2.3. Biofilm formation

2.2.3.1. Fluorescent *in situ* hybridization and confocal laser scanning microscopy. To observe biofilm formation as well as yeast and bacterial species co-occurrence patterns within the biofilm, fluorescent *in situ* hybridization (FISH) with different fluorochromes was used to specifically monitor the main microbial groups by confocal laser scanning microscopy (CLSM) at the microscopy platform "Plateforme d'Imagerie et de Mesures en Microscopie (PIMM)", University of Bretagne Occidentale. Probes to specifically target yeasts (EUK516) and bacteria (EUB338) but also AAB (ALF1B) and LAB (LGC and Ooeni) were synthesized with different fluorochromes (Table S1). Preliminary FISH tests were performed on the eleven strains of the defined consortium using EUB338, EUK516, ALF1B and LGC probes to confirm cell fixation, probe hybridization and specificity.

For biofilm observations by CLSM, cell fixation was performed with protocol described by Roller, Wagner, Amann, Ludwig, and Schleifer (1994). An approximately 15 mm² sample was cut and transferred into a tube with 500 µL PBS (PBS; 130 mM NaCl, 10 mM Na₂HPO₄/NaH₂PO₄, pH 7.2-7.4) and 500 µL ice-cold 96% ethanol then conserved at -20 °C until hybridization. For cell hybridization, protocol adapted from Manz, Amann, Ludwig, Wagner, and Schleifer (1992) was applied. To do so, samples were transferred into 8-wells microscopy slides (Ibidi, Germany) and dried and dehydrated by directly adding and removing 300 µL of 50%, 80% and 96% ethanol in the well. 100 µL of hybridization buffer (20% formamide) were deposited to completely immerse the sample and 12 µL of probe solution (25 ng/µL) were added, then the slides were incubated at 46 °C for 4 h (humidity equilibrated).

Afterwards, each slide was washed by immersion in a washing buffer (freshly prepared using 0.225 M NaCl, 20 mM Tris-HCl and 0.01% SDS pre-heated to 48 °C) for 10 min at 48 °C in a water bath. Finally, slides were very briefly washed with ice-cold distilled water and dried with compressed air. One drop of anti-fade solution (ProLong Diamond Antifade Mountant, Thermo Fisher Scientific, USA) was deposited on the surface of each sample and the slides were kept at -20 °C in darkness until microscopy observations. Labeled biofilm samples were analyzed by using a confocal microscope ZEISS LSM780 using the different probes at the wavelengths indicated in Table S1. Three biological replicates were treated per sample and at least two were analyzed.

2.2.3.2. Scanning electron microscopy. As for CLSM, biofilms were transferred into tubes containing 1 mL of fixing solution (50 mL of cacodylate buffer pH 5 (cacodylate solution 0.4 M adjusted to pH 5 with 0.2 M hydrochloric acid), 10 mL of glutaraldehyde 25% and 40 mL of sterile distilled water) for 30 min. Samples were washed twice with 2-fold diluted cacodylate buffer and conserved overnight. Dehydration was performed by successive baths in 50%, 70%, 90% and 100% ethanol for 3 min each, with drying in between. Finally, each sample was placed on a glass slide and incubated at 35 °C until metallization by a gold sputter-coater and Scanning Electron Microscopy (SEM; HITACHI S-3200 N).

2.2.4. Metabolome

2.2.4.1. Organic acid quantification by liquid chromatography-quadrupole-time-of-flight mass spectrometry (LC-Q-TOF) and enzymatic kits. Filtered tea samples were transferred into amber vials then 2 µL were injected into a HPLC 1260 coupled to a 6530 Accurate-Mass quadrupole-time-of-flight mass spectrometry Q-TOF (Agilent Technologies, Santa Clara, CA) equipped with a dual electrospray ionization source (Agilent Technologies, Santa Clara, CA) based on the previously described protocol (Ibáñez & Bauer, 2014). Molecules were separated using a Phenomenex (Torrance, CA) Rezex ROA-Organic Acid H+ (8%) (300 × 7.8 mm) column equipped with a Rezex ROA-Organic Acid H+ (8%) (50 × 7.8 mm) guard column and analytes were ionized in negative electrospray ionization (ESI-) mode in a scan range of 50 to 1700 *m/z* and 2 scan/s. The column was maintained at 55 °C with an isocratic flow rate of 0.3 mL/min of water containing 0.1% formic acid (LC/MS grade Carlo Erba Reagents, France) while samples were maintained at 10 °C in a well plate autosampler until injection. Run time was 15 min followed by 5 min post-time to wash and re-equilibrate the column before the next injection. The mass spectrometer conditions were as follows, capillary voltage 4000 V, source temperature 325 °C, nebulizer pressure, 50 psig, drying gas, 1 L/min.

Stock solutions of five organic acids (Table S2) were prepared in water supplemented with 0.1% formic acid and a 10-point linear range was prepared at a concentration between 0.01 and 100 µg/mL. Standard solutions were first injected separately (three injections) to confirm accurate identifications with the theoretical mass-to-charge (*m/z*) values (Table S2), then in a mixture to validate peak separation and retention times and determine limits of detection and quantification. MassHunter Quantitative Analysis software version B.07.01 (Agilent Technologies) was used for compound identification and quantification using the ions listed in Table S2.

For acetic and lactic acids, concentrations were determined using the Acetic acid, UV method and Enzytec Liquid D/L-lactic acid enzymatic kits (r-biopharm, Germany) according to manufacturer's instructions.

2.2.4.2. Ethanol quantification. Ethanol quantification was performed by gas chromatography using a GC 3900 (Varian Analytical Instruments, USA) equipped with a CP Sil 8CB LB/MS #CP8752 column (30 m × 0.32 mm, FT 0.25 µm, Chrompack Capillary Column, Varian, USA), an FID detector and an EFC detector as described by Coton et al., 2017. Results

were expressed in g/L.

2.2.4.3. Volatile compound profiles by gas chromatography-mass spectrometry. Each sampling day, 2.5 ± 0.02 g of Kombucha tea samples were transferred into 22-mL Perkin Elmer vials, tightly sealed and kept at -20 °C until analysis. Volatiles were extracted and analysed by headspace (HS) trap extraction coupled to gas chromatography-mass spectrometry (GC-MS) using a Perkin Elmer Turbomatrix HS-40 trap automatic headspace sampler with trap enrichment and a Clarus 680 gas chromatograph coupled to a Clarus 600 T quadrupole mass spectrometer (PerkinElmer, France), as previously described (Pogačić et al., 2015), with modifications of the chromatographic conditions according to Penland et al. (2020). The samples were injected in a random order, with standards and blank samples (boiled deionized water) to monitor possible carryover and MS drift. Volatile compounds were identified by comparing their retention index and mass spectra with those from the NIST 2008 Mass Spectral Library (Scientific Instrument Services, Ringoes, NJ, United States) and, when possible, with those of authentic standards (Sigma Aldrich, France) analyzed in the same conditions.

2.2.4.4. Statistical and correlation analyses. Statistical analyses were performed using the R software (R Core Team, 2019, 2019).

Analyses of variance (ANOVA) and mean comparison were used to determine whether the physico-chemical, microbial and biochemical data significantly changed during the time-course of fermentation.

Data from GC-MS were centered and scaled by compound and hierarchically clustered by Ward's minimum variance method and Euclidean distance metric with the *hclust* R function before being plotted by the *heatmap.2* function of R *gplots* package. Principal component analysis (PCA) was first used to identify common biochemical profile changes over fermentation times using tea and biofilm data. Then, a multiple factor analysis (MFA) was performed using the MFA function of the *FactoMineR* package (Lê, Josse, & Husson, 2008). The data set was constituted of three groups of active variables: pH and density, concentrations of eight organic acids and log values of abundance of 39 volatile compounds from GC-MS analysis plus ethanol from HPLC, for the triplicate samples from d7 to d27. The age of samples and the 25 variables from both culture-dependent and -independent microbial analysis of tea and biofilm were used as supplementary (i.e. illustrative) variables. All analyses were performed with R software using *FactoMiner*, *Factoextra*, *Hmisc*, *Psych* and *gplots* packages (Lê et al., 2008; Wickham, 2016).

3. Results

3.1. Physico-chemical analyses

pH quickly decreased from an initial value of 5.57 to 3.40 ± 0.04 during the first seven days then progressively reached 3.02 ± 0.05 by day 27 (Fig. 1). Density values also decreased quickly during the first 11 days from 1018 to 1010 ± 0.58 then stabilized between 1010 and 1008 until the end of the fermentation (Fig. 1) as sugars were consumed by the consortium.

Biofilm formation was monitored over time and a relatively thin biofilm quickly appeared on the tea surface (first 7 days), with a wet mass of 2.27 ± 0.15 g. It progressively darkened, strengthened and thickened to reach a wet mass of 5.36 ± 0.1.12 g by d27. The biofilm mass increased with a rate calculated at 0.32 g/day during the first 7 days, then 0.15 g/day up to d27 (Fig. 1).

3.2. Microbial populations monitored by culture-dependent analyses

In tea samples, microbial counts significantly increased by nearly 2 log₁₀ CFU/mL during the first 7 days, from 5.82 to 7.35 ± 0.05 log₁₀ CFU/mL for yeast populations, 6.30 to 8.74 ± 0.11 log₁₀ CFU/mL for

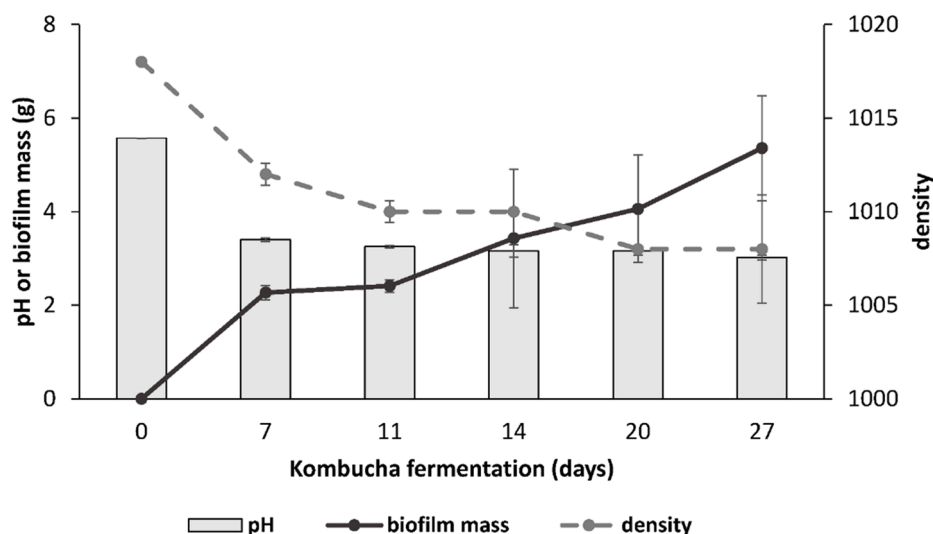


Fig. 1. Results of physico-chemical parameters followed during 27 days Kombucha fermentations. The pH and density were determined in the tea fraction at day 0, 7, 11, 14, 20 and 27 as well as the biofilm mass. Results correspond to the average of three biological replicates with standard deviations.

AAB and from 6.76 to $7.64 \pm 0.08 \log_{10}$ CFU/mL for LAB (p value ≤ 0.01) (Fig. 2). In some cases, slightly higher concentrations than those expected for AAB and LAB can be explained by overestimations using the OD600nm-CFU/mL calibration curves. Yeasts and AAB populations were significantly higher at 7 days compared to the following days, then progressively decreased up to 27 days ($6.93 \pm 0.06 \log_{10}$ CFU/mL and $7.39 \pm 0.05 \log_{10}$ CFU/mL respectively), with an observed increase from 11 to 14 days (p value = 0.06 and 0.01, respectively), while the LAB populations remained stable from 7 to 20 then significantly decreased up to 27 days ($7.40 \pm 0.14 \log_{10}$ CFU/mL, p value = 0.02). Biofilm populations were significantly higher than those in tea for both bacteria and yeasts. Yeast and LAB populations remained relatively stable during the fermentation at nearly $8.7 \log_{10}$ CFU/g and $7.5 \log_{10}$ CFU/g respectively. On the other hand, AAB populations were highly active and significantly increased from 7 to 14 days ($7.5 \pm 0.15 \log_{10}$ CFU/g to $9.9 \pm 0.60 \log_{10}$ CFU/g, p value = 0.003) then significantly decreased to $8.8 \pm 0.07 \log_{10}$ CFU/g at 27 days (p value = 0.04) (Fig. 2). Moreover, no visible contamination (e.g. molds) was observed during all fermentations.

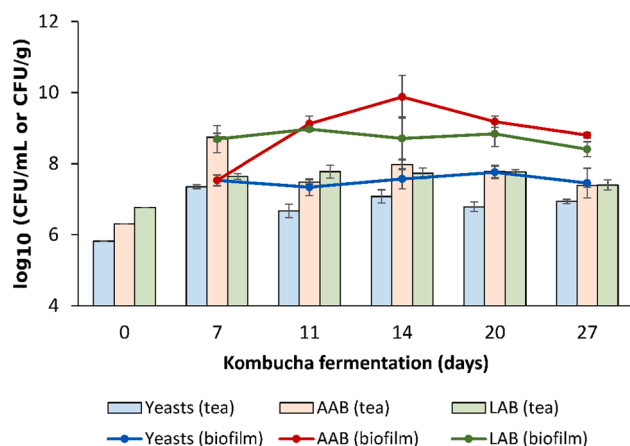


Fig. 2. Numeration of bacteria and yeasts during Kombucha fermentation in tea and biofilm. Yeasts, acetic acid bacteria (AAB), lactic acid bacteria (LAB) were numerated at days 0, 7, 11, 14, 20 and 27 in tea and biofilm except d0 for this latter. Results correspond to the average of three biological replicates with standard deviations and expressed as \log_{10} CFU/mL (tea samples) or \log_{10} CFU/g (biofilm samples).

3.3. Dynamic changes in bacterial and fungal consortium species determined by 16S rRNA and 26S metabarcoding analyses

Metabarcoding analyses were performed to monitor the relative abundance of bacterial (Fig. 3A) and yeast (Fig. 3B) species in tea and biofilm samples throughout fermentation. Concerning bacterial community structure, *A. okinawensis* and *L. nagelii* were dominant in tea samples throughout the fermentation (41 to 56% and 39 to 57% of the abundance respectively) while other AAB and *O. oeni* were at lower relative abundances. In the biofilm, *A. okinawensis* was the most dominant species throughout the fermentation (65 to 93% of the abundance), followed by *L. nagelii* (2 to 17% of the abundance) and the three other AAB species (*K. Hansenii*, *G. oxydans*, *A. tropicalis*). The latter species' relative abundances increased during the course of fermentation and represented ~ 20% of the biofilm bacterial microbiota at the end of fermentation (Fig. 3A). Beta-diversity analyses confirmed these observations as shown in Fig. S1 in which a Principal Coordinate Analysis (PCoA) based on Bray-Curtis distance at the species level is plotted. Indeed, bacterial communities were grouped together as a function of sample type, i.e., tea or biofilm (Adonis test, $p < 0.001$, $R^2 = 0.802$), while fermentation time shaped beta-diversity among biofilm bacterial communities (Adonis test, $p < 0.005$, $R^2 = 0.619$) but not that of tea bacterial communities (Adonis test, $p > 0.05$). Concerning yeast community structure, both tea and biofilm sample types harbored similar community structures (Fig. 3B and S1, Adonis test, $p > 0.05$) and were dominated by *D. bruxellensis* and *H. uvarum* throughout fermentation. Interestingly, a shift in the dominance of these species was observed during fermentation as *H. uvarum* dominated up to d14 and d20 in the tea and biofilm, respectively, while *D. bruxellensis* dominated the latter fermentation stages. Indeed, for both sample types, it was found that fermentation time (Adonis test, $p < 0.001$, $R^2 = 0.742$) shaped yeast community structure based on Bray-Curtis distances.

3.4. Biofilm formation by the complex consortium monitored during fermentation

Preliminary tests using FISH confirmed that the selected protocol did not require any enzymatic permeabilization (lysozyme) step on the fixed cells, using either pure cultures or biofilm samples, and probe specificities (Fig. S2A, B, C). Yeasts and bacteria were differentiated using simultaneous hybridizations with two different fluorochromes. Interestingly, the biofilm negative control (without probes) showed natural fluorescence in CLSM, probably due to its cellulose composition.

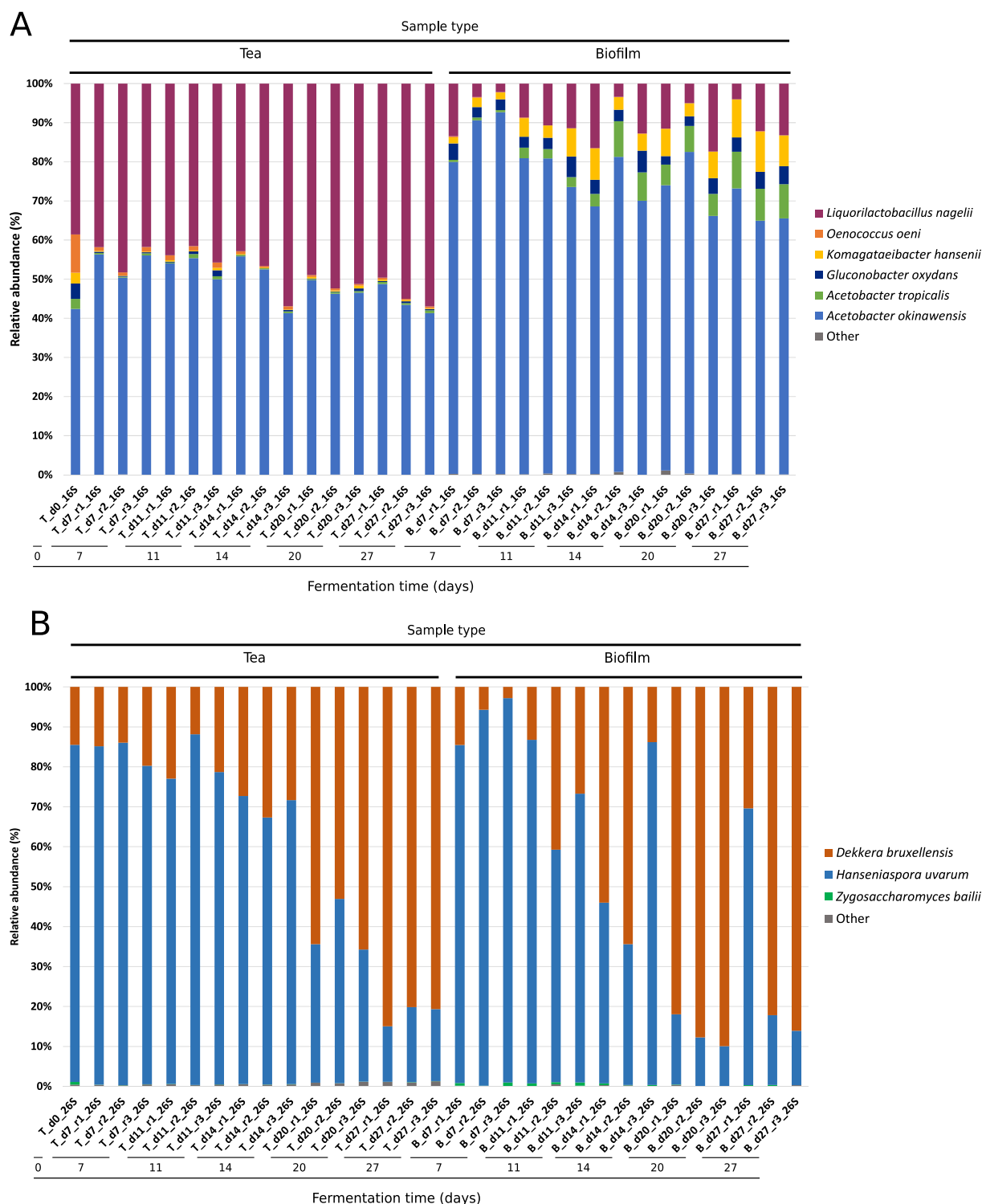


Fig. 3. 3A and 3B. Relative abundances of bacterial (A) and yeast (B) species throughout Kombucha fermentation. Each replicate is represented in both tea (T) and biofilm (B) as r1, r2 and r3 for each sampling date 0, 7, 11, 14, 20, 27 days (d0, d7, d11, d14, d20 and d27).

Dynamic monitoring of biofilm formation by the tailor-made consortium highlighted distinct bacteria and yeast cell clustering patterns as the structure strengthened and thickened (Fig. 4A to L). There was a high abundance of bacterial cell clusters, certainly linked to the highly active AAB populations in biofilm samples, in comparison to yeasts, although no specific biofilm structure was observed. Microscopy observations at different sampling times showed yeast cells frequently entrapped and/or completely covered by bacterial cells which can likely

explain the difficulty to observe them in some acquisitions. In Fig. 4E, d7 biofilm showed that yeasts were mainly grouped on the outer surface of the biofilm, although impossible to determine whether this section was in direct contact with the air or tea (due to orientation loss during treatment). After 11 days fermentation, yeast and bacterial cells were more organized and a bacterial mat was observed covering yeast cell clusters (Fig. 4F), this same observation was made on all 3 biological replicates. This finding reinforced the idea that symbiotic relationship

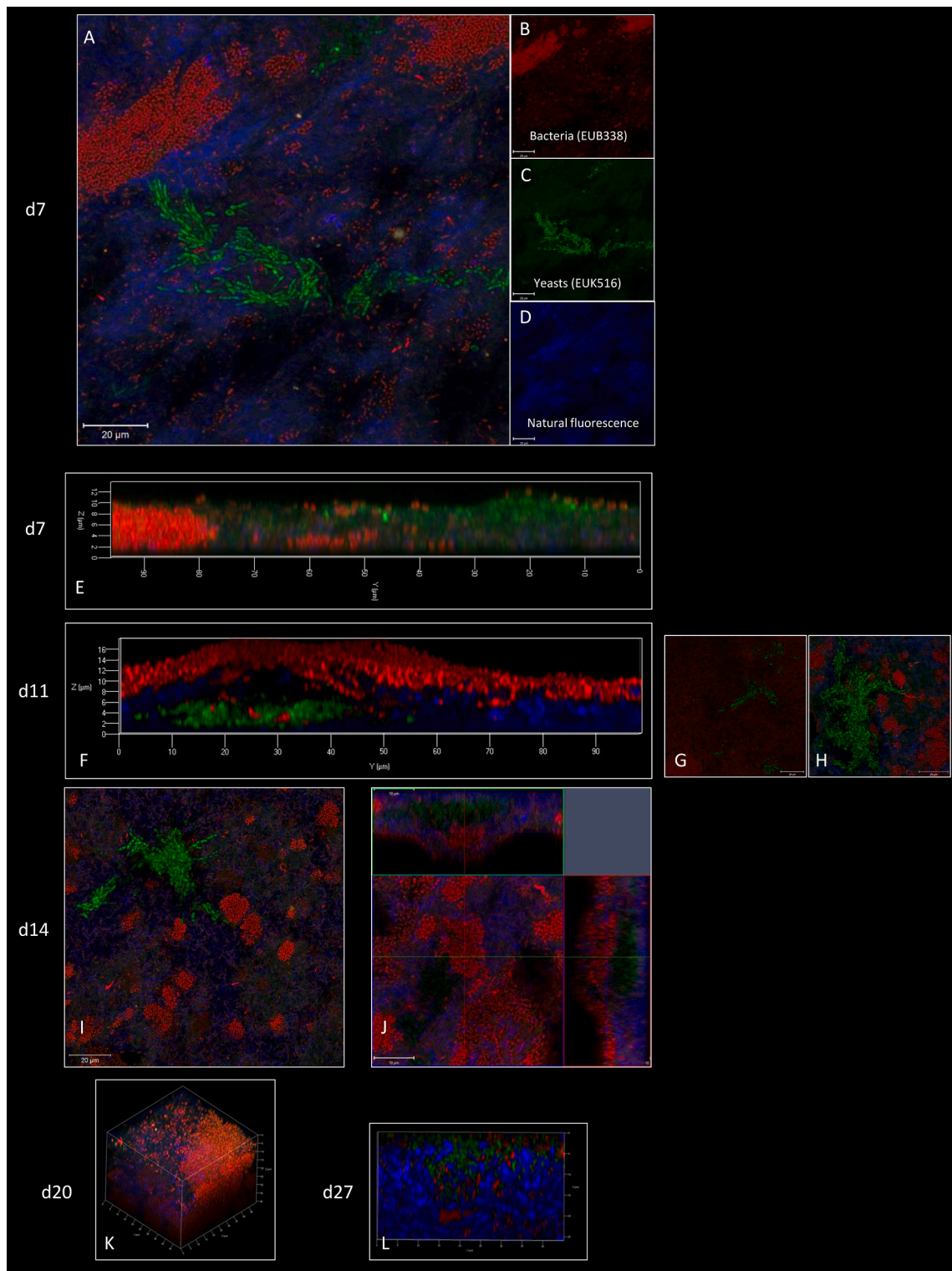


Fig. 4. Dynamic monitoring of biofilm formation by confocal laser scanning microscopy using fluorescent *in situ* hybridization. The figures A to L correspond to CLSM acquisition changes in biofilm during fermentation at days 7, 11, 14, 20 and 27 (d0, d7, d11, d14, d20 and d27). The natural fluorescence of the biofilm is represented in blue in these acquisitions (e.g. Fig. 4D) while specific hybridizations with probes targeting bacteria (EUB338) and yeasts (EUK516) are represented in red (e.g. Fig. 4B) and green (e.g. Fig. 4C), respectively. Fig. 4A, 4B, 4C, 4D, 4G, 4H, 4I were obtained on the same focal point (z) while Fig. 4E, 4F, 4K and 4L were obtained in depth of samples and the Fig. 4J was obtained with both methods. (For interpretation of the references to color in this figure legend, the reader is referred to the web version of this article.)

and cooperative metabolism between these microbial populations may exist in the biofilm during fermentation. Obviously, biofilm density depended on the observed zone and depth as represented in Fig. 4G and 4H. At d14, this phenomenon was accentuated, and bacteria and yeasts were very abundant (Fig. 4I and 4J). Then, a major increase in biofilm, concomitant with a progressive decrease in bacteria and yeast clusters, was observed at days 20 and 27 (Fig. 4K and 4L). Specific probes

targeting AAB and LAB (with a specific probe for *O. oeni* due to the lack of fluorescence with the LGC probe, which can be explained by two mismatches on 16S rRNA gene target) were also used on these samples but no further differences were found (Fig. S3). Finally, LAB cells were certainly present but at much lower levels or scattered, so less accurately observed (Fig. S3).

SEM observations were consistent with CLSM observations (Fig. 5).

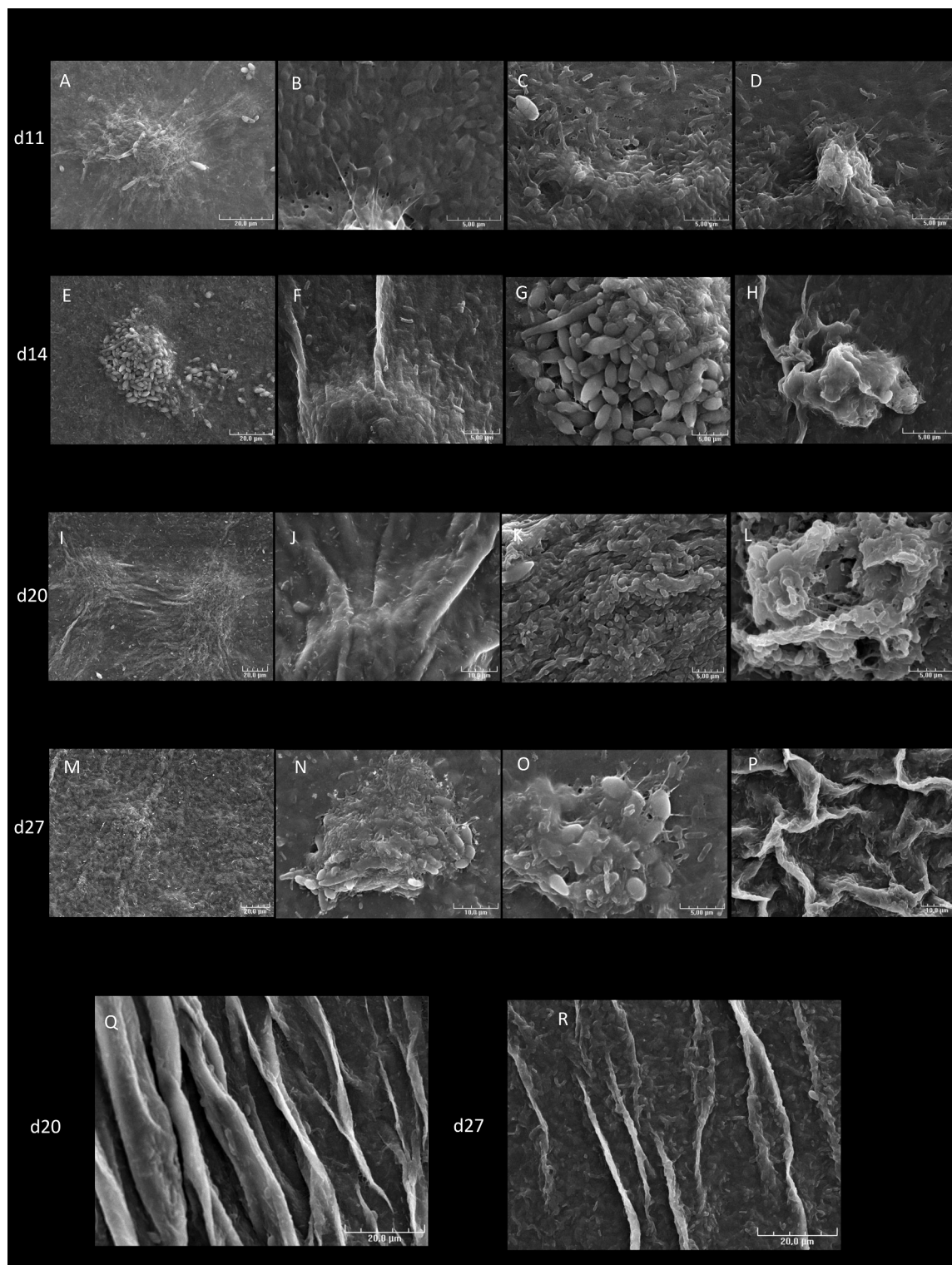


Fig. 5. Dynamic monitoring of biofilm formation by Scanning Electron Microscopy. The figures correspond to SEM acquisitions showing changes in biofilm during fermentation at days 11 for figures A to D, 14 for E to H, 20 for I to L and 27 for M to P and finally Q and R corresponds to days 20 and 27.

Indeed, yeast cells were grouped in clusters (based on cell shapes, consortium species could even be distinguished) (Fig. 5A, 5E, 5I and 5M) and progressively covered by increasingly abundant bacterial cells during the fermentation (Fig. 5A, 5B, 5C, 5E, 5F, 5G, 5I, 5J, 5K, 5M and 5O). Biofilm matrix also densified, clearly embedding bacterial and yeast cell clusters within its structure by d11 to the end. Also, between d20 and d27, microorganisms were observed to be in curly shaped fibrils that could be distinctly seen throughout the biofilm samples (Fig. 5Q and 5R). Interestingly, several pores were also observed on the surface of the biofilm at d11 with fibrous extensions (Fig. 5B and 5C) appearing from and around bacterial cells and embedding the yeast cells thus creating a strengthening network from the bacterial cellulose being produced over time (Fig. 5D, 5H, 5L and 5P). Finally, on some SEM acquisitions, biofilm production appeared to be linked to yeast cells (Fig. 5O), although it could be an artefact of cellulose produced by AAB.

3.5. Changes in organic acids and ethanol content during fermentation

Seven organic acids were quantified in Kombucha tea samples during fermentation with very significant variations in concentrations for succinic, oxalic, malic, glucuronic and gluconic acids (p value < 0.001). At the start, only three acids were quantified while by d7 all organic acids were present except glucuronic acid that was only quantified from d11 onwards (Fig. 6A). Concentrations of gluconic, glucuronic, malic, oxalic and succinic acids then significantly increased until d20 before stabilizing to concentrations of 0.027 ± 0.006 g/L, 0.021 ± 0.004 g/L, 0.003 ± 0.001 g/L, 0.020 ± 0.005 g/L and 0.015 ± 0.004 g/L, respectively (Fig. 6A). As expected, acetic and lactic acids were observed at 10 to 1000-fold higher concentrations than the other acids (Fig. 6B). Acetic acid was quantified at variable concentrations between d7 (1.31 ± 0.04 g/L) and d20 (1.45 ± 0.07 g/L) (p value = 0.0906), then increased to 2.41 ± 0.06 g/L at d27 (Fig. 6B). Lactic acid was quantified at 318 ± 42 μ g/mL at d7 and significantly increased to reach 0.82 ± 0.02 g/L at d20 before decreasing to a final concentration of 0.45 ± 0.02 g/L (Fig. 6B).

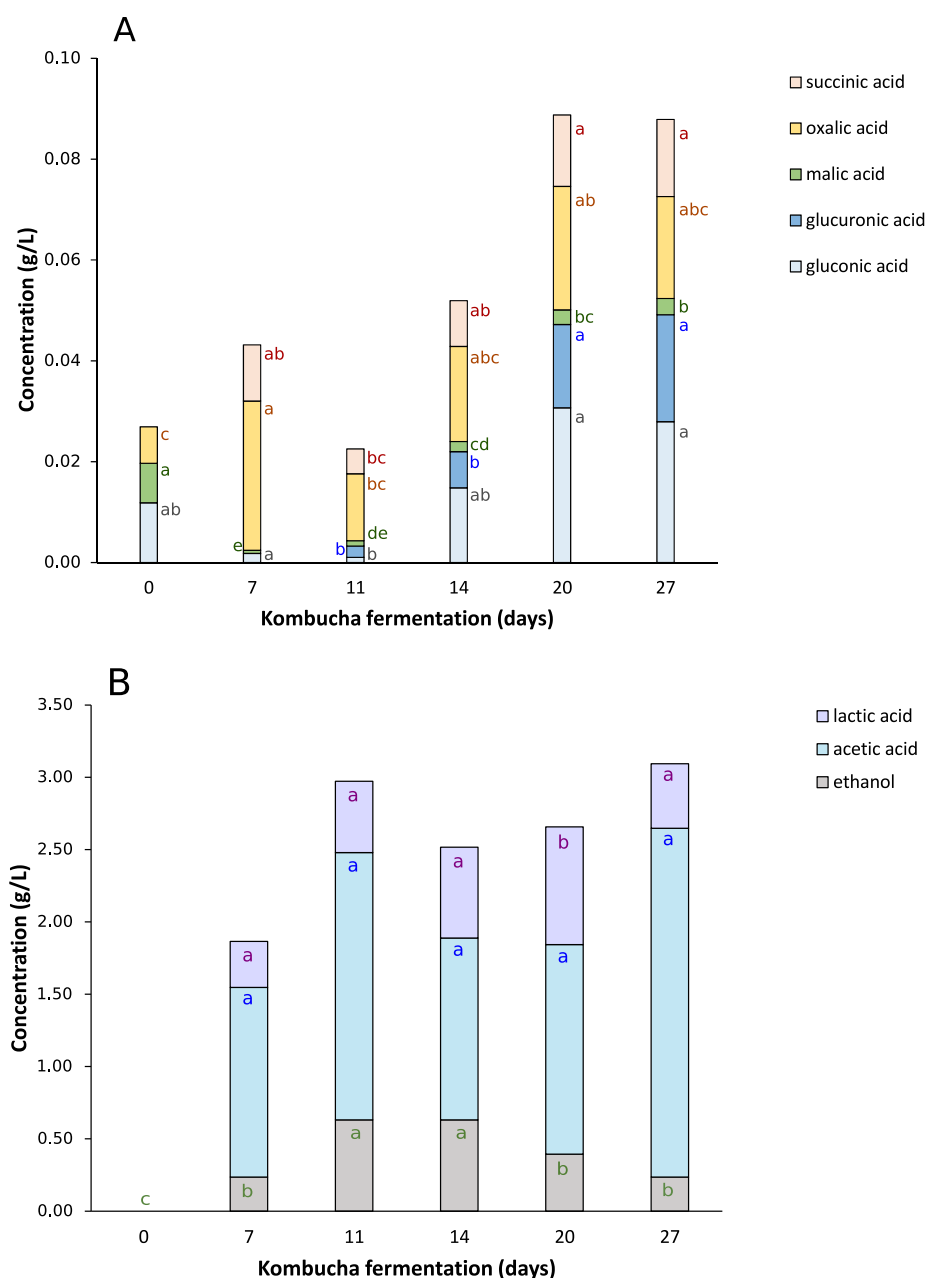


Fig. 6. Changes in organic acids concentrations during Kombucha fermentations. Gluconic, glucuronic, malic, oxalic and succinic acids were quantified by LC-MS method (6A) while acetic and lactic acids were quantified by enzymatic kits (6B) and ethanol by GC. Organic acids concentrations in g/L of Kombucha (tea) were quantified at 7, 11, 14, 20 and 27 fermentation days. The letter appearing corresponds to the results of the comparing means tests. The results correspond to the averages of three biological replicates.

Finally, ethanol was mainly produced between d0 and d11 and showed a significant increase from 0.237 g/L (± 0.010) (d7) to 0.631 g/L (± 0.126). Concentrations then progressively decreasing to the end of fermentation to each 0.237 g/L (± 0.066). Ethanol content was systematically below 0.789 g/L during fermentation (Fig. 6B).

3.6. Changes in the volatilome during fermentation

A total of 39 volatile compounds were identified and belonged to eight main families: alcohols ($n = 6$), aldehydes ($n = 6$), carboxylic acids ($n = 4$), esters ($n = 11$), fatty acids ($n = 6$), furans ($n = 1$), ketones ($n = 4$) and styrene (Table S3). The heat-map drawn from hierarchical clustering analysis (Fig. 7) as well as the principal component analysis (Fig. S4) show the main changes in volatile compound abundances over time with good repeatability, as the three biological tea replicates were systematically grouped, and samples were distinguished at the six time points with specific compounds being produced or most abundant. Moreover, the heat-map highlighted four clusters (A, B, C, D on Fig. 7) also observed on the PCA. Indeed, cluster B ($n = 4$) contained three aldehydes and butan-2-ol that tended to show high abundances at d0 or that did not show significant changes over time, then cluster A ($n = 8$) corresponded to volatiles that were most abundant at d7, d11 and/or d14 before decreasing, such as nonanal and dodecanal. The volatilome complexified after d11 and d14 which corresponds to the standard fermentation time for this product and this is represented as cluster D ($n = 19$) on the heat-map. Different alcohols (e.g. 2-methylpropan-1-ol, 3-methylbutan-1-ol) were produced as well as some fatty acids (e.g. octanoic and hexanoic acids) and ethyl esters (e.g. ethyl heptanoate, ethyl-2-methylbutanoate). In the last fermentation stages, as highlighted in cluster C ($n = 8$), some volatile compounds became increasingly abundant between d20 and d27, such as different acids (e.g. acetic, 4-hydroxybutanoic acids), ketones (e.g. hexan-2-one and heptan-2-one) and some specific esters (3-methylbutyl acetate, ethyl propanoate).

3.7. Microbiota and biochemical profile correlation during fermentation

A multiple factor analysis (MFA) was performed to have a global

view of the changes occurring during Kombucha fermentation and to illustrate the correlations between microbial and biochemical variables. A total of 74 physicochemical (pH, density, organic acids, volatiles) and microbial (counts and metabarcoding) parameters were included, which described both the tea and biofilm samples from d7 to d27. Dimensions 1 and 2 respectively explained 49.7% and 18.5% of the total variance and separated samples according to time in three clusters: d7, d11-d14, and d20-d27 samples, (Fig. 8). The beginning of the fermentation (d7 samples) was characterized by high density and pH values, high concentration of several aldehydes, correlated to the greatest AAB counts in tea and the highest abundances of three of the nine species included in the tailor-made consortium: the yeast *H. uvarum* both in tea and biofilm, the LAB *O. oeni* in tea and the AAB *Z. bailii* in biofilm. Days 11 and 14 were correlated to AAB counts in biofilm and numerous compounds including ethanol, many ethyl esters and diacetyl (2,3-butanedione). The final fermentation stage, between d20 and d27, was associated with higher abundances of glucuronic, gluconic and malic acids and some volatiles, including branched-chain acids and esters (e.g. 2-methylpropanoic acid, 3-methylbutanoic acid, 3-methylbutyl acetate and ethyl propanoate) and methyl ketones and secondary alcohols (e.g. hexan-2-one and hexan-2-ol). These changes were correlated to a high biofilm mass, high abundances of *D. bruxellensis* in both tea and biofilm and of *A. tropicalis* in biofilm.

4. Discussion

Kombucha is an ancient naturally fermented beverage that has become increasingly popular in the Western world. Many recent studies have described the microbial communities encountered in the fermented tea and/or biofilm used as backstop using culture-dependent and -independent approaches. The main metabolites produced as well as the potential antimicrobial properties or health benefits of the fermented drink have also been documented. However, the Kombucha microbiome and related properties depend on several parameters. The biofilm backstop used for successive spontaneous fermentations is portioned and often shared among producers. Its microbial stability and maintenance have yet to be fully investigated and changes in microbial composition

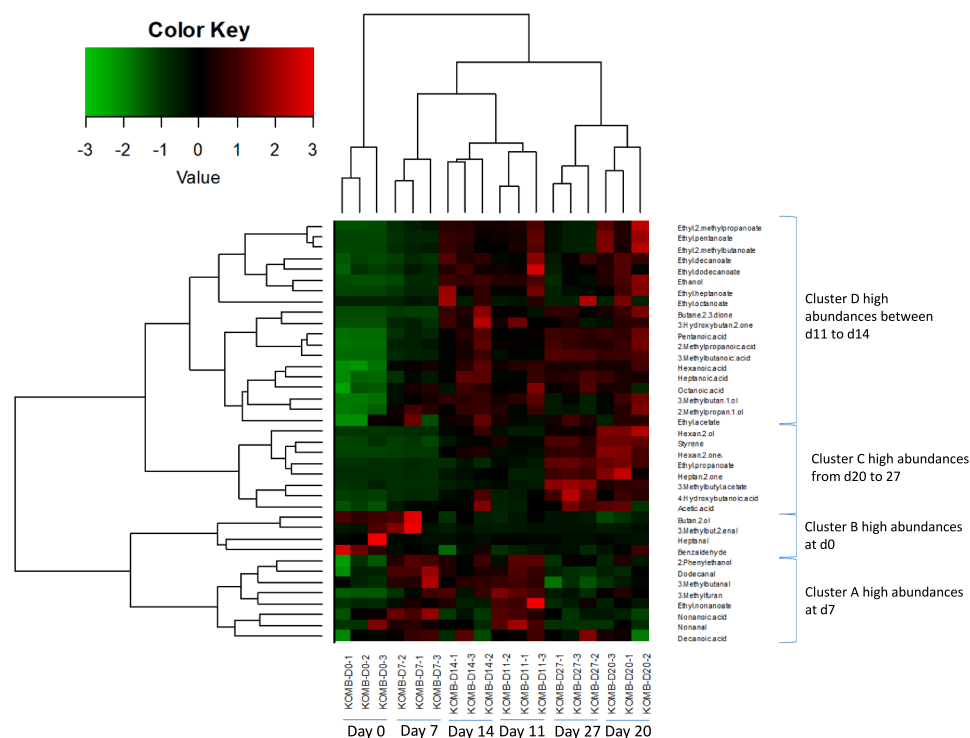


Fig. 7. Normalized heat-map representation of changes in Kombucha volatilome during fermentation. Hierarchical clustering was done using Ward's linkage and Euclidean distances. Sample names and fermentation times are provided on the bottom and volatile compound names on the right side as well as the four clusters. The green to red color range indicates low to high compound abundances. (For interpretation of the references to color in this figure legend, the reader is referred to the web version of this article.)

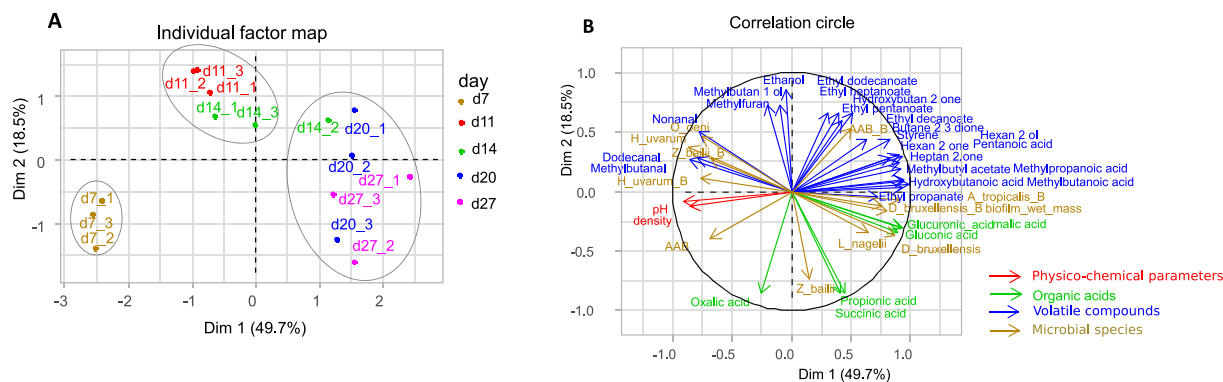


Fig. 8. Multiple factor analysis performed on samples collected at d7, d11, d14, d20 and d27 with three groups of active variables: pH and density, organic acid concentrations and abundance of 39 volatile compounds. Individual factor map (A) and variable factor map (B). Microbial data from culture-dependent ($n = 6$) and -independent ($n = 18$) analyses of tea and biofilm and biofilm wet mass were used as supplementary variables. The ellipses on plot (A) show the three groups from agglomerative hierarchical clustering on results from MFA. The variables poorly represented on plot (B) are not shown ($\cos^2 < 0.5$).

over time are likely to occur. Fermentation can also vary due to differences in tea type, production conditions (e.g. tank size, oxygen availability, temperature...) and, to a lesser extent, geographical origin. To date, Kombucha fermentations largely rely on the autochthonous microbiota embedded within the biofilm, with new layers generated during each fermentation, or the in-house microbiota coming from the production environment or equipment. During successive fermentations, batch-to-batch variations can be therefore observed and are typically linked to changes in the Kombucha microbiome and abundances of the main fermentation drivers. In this context, selection of the key microbial drivers from the Kombucha core microbiota is of clear interest to drive and better control this fermentation. The main objectives of this study were to design a tailor-made complex consortium including species belonging to this core microbiota, as recently described by [Coton et al. \(2017\)](#), and evaluate its impact on fermentation by monitoring multiple physico-chemical, biochemical, microbial and biofilm parameters. The tailor-made consortium included nine yeast, AAB and LAB species considered as the main drivers, including two involved in biofilm formation (*K. hansenii* and *G. oxydans*).

Kombucha fermentations typically take up to 15 days and our data were consistent with this timeframe as both density and pH reached target values during the first 14 days (density ~ 1010 and pH ~ 3.2). However, we extended fermentation time to 27 days to monitor biofilm formation as it was solely produced by the tailor-made consortium. Biofilms can be considered to be complex associations of one or more species interconnected cells embedded within a self-produced matrix and formed at either solid-liquid or liquid-air interfaces ([Alexandre, 2013](#); [Costerton, Lewandowski, Caldwell, Korber, & Lappin-Scott, 1995](#); [Hall-Stoodley, Costerton, & Stoodley, 2004](#); [Kolter & Greenberg, 2006](#)). A thin biofilm was rapidly observed at the liquid-air interface and covered the entire tea surface within 7 days, then progressively thickened and darkened to the end of fermentation.

All microbial groups developed well in tea samples (up to +2 log increase in the first 7 days), as shown by microbial numerations, and these changes were linked to the rapid decrease in pH due to organic acid production, in particular acetic and lactic acids, by the consortium. These findings are in accordance with previous culture-dependent data including the same species described by [Coton et al. \(2017\)](#). AAB populations were particularly active in the floating biofilm as the highest population increase was observed for this group. This can be directly linked to their obligately aerobic metabolism and the oxidative transformation of ethanol into acetic acid. Some AAB species as *Acetobacter pasteurianus* can also oxidize lactic acid released by LAB into acetic acid and acetoin ([Moens, Lefeber, & De Vuyst, 2014](#)). AAB species involved in biofilm formation are also most likely using this strategy to increase their access to oxygen as recently described by [May et al. \(2019\)](#).

Similar results were also observed with microscopy observations as

the microbiota was progressively embedded in the newly formed biofilm structure, especially AAB and yeasts. To the best of our knowledge, this is actually the first time that Kombucha biofilm formation is dynamically followed and observed using FISH probes coupled to CLSM and SEM. The only studies using CLSM on SCOBY were performed with non-specific probes such as calcofluor or thiazine ([Podolich et al., 2017](#); [Reva et al., 2015](#)). Here, we used yeast- and bacteria-specific probes with distinct fluorochromes to decipher microbial co-occurrence patterns in the newly created biofilm. One drawback should be noted as there is a loss in biofilm orientation during treatment. Dynamic follow-up by FISH coupled to CLSM showed no particular cell configuration within the biofilm except for AAB, which clearly dominated and progressively surrounded large yeast clusters. These cell interactions most likely enhance the symbiotic relationship and cooperative metabolism that occurs between the main microbial drivers during fermentation. SEM observations confirmed and even completed this observation and the biofilm constituents appeared to be actively secreted from some bacterial cells. *Gluconacetobacter* spp. ([Mikkelsen, Flanagan, Dykes, & Gidley, 2009](#); [Zhang, Wang, Qi, Ren, & Qiang, 2018](#)) and, in particular, *K. xylinus* (formerly *G. xylinus*) ([Yamada et al., 2012](#)) or *K. hansenii* (formerly *G. hansenii*) ([Hodel et al., 2020](#)), have all been described to produce biofilms and, as mentioned, our tailor-made consortium included biofilm-producing *K. hansenii* and *G. oxydans* strains (an easily observable trait in liquid cultures). Interestingly, comparable microscopic observations have already been made in other studies. [Dima et al. \(2017\)](#) studied a natural biofilm with similar composition (species belonged to *Komagataeibacter*, *Gluconobacter Zygosaccharomyces*, *Bretanomyces*, *Pichia* genera but also included some LAB) and observed a cellulosic cluster although bacteria and yeasts could not be accurately distinguished. In addition, [El-Taher \(2011\)](#) also performed analyses on a biofilm containing *P. occidentalis* and *K. xylinus* and both were clearly embedded in the biofilm. Interestingly, SEM observations on biofilms produced from pure cultures (*K. xylinus* or *K. hansenii*) clearly highlighted a more organized cellulosic network with several fibrils and no apparent presence of embedded bacteria ([Gromovkykh et al., 2020](#); [Mikkelsen et al., 2009](#); [Zhang et al., 2018](#)). Such observations suggest that other microbial interactions exist between bacteria and yeasts within the Kombucha biofilm and the resulting biofilm may be different according to the species present. Yeasts and LAB ([Edwards, Collins, Lawson, & Rodriguez, 2000](#)) may also produce biofilms or participate in its production. The biofilm mode of life of the wine spoilage yeast, *D. bruxellensis*, has been recently described and may be linked to a potential resistance strategy to persist in the winemaking environment or in wines ([Lebleux et al., 2020](#)). In Kombucha, this species is a key driver of the fermentation and may play a participative role in biofilm formation, together with biofilm-producing AAB. Our microscopic observations suggest biofilm filaments were released from some yeast cells

meaning at least one or more yeast species can produce it during fermentation. Yeast biofilm production, in particular for *Dekkera/Brettanomyces* as well as *Saccharomyces* or *Debaryomyces* species, has already been described in co-cultures with LAB species (Furukawa, Yoshida, Ogihara, Yamasaki, & Morinaga, 2010; Kawarai, Furukawa, Ogihara, & Yamasaki, 2007; León-Romero, Domínguez-Manzano, Garrido-Fernández, Arroyo-López, & Jiménez-Díaz, 2016; May et al., 2019). Noteworthy, *L. nagelii* dextran production from sucrose has also been reported (Edwards et al., 2000) and despite the fact we could not observe *L. nagelii* clusters in the biofilm, LAB species, which reached $> 8 \log_{10}$ CFU/g biofilm, were detected using 16S rRNA gene metabarcoding so its role in biofilm formation cannot be excluded. Furthermore, in a recent study focusing on the interactions of *L. nagelii* and *Saccharomyces cerevisiae* encountered in water kefir, it was found that *L. nagelii* profits from amino acids (i.e., glutamine, histidine, methionine, and arginine) and riboflavin released by *S. cerevisiae* (Bechtner, Xu, Behr, Ludwig, & Vogel, 2019). If the Kombucha microbiota is well embedded in this biofilm structure, it can be clearly assumed that cooperative metabolism takes place and is even facilitated. Further work would therefore be necessary to provide a deeper understanding of the interactions occurring between yeasts, AAB and LAB.

We also observed many distinct biochemical changes during fermentation. As mentioned, yeasts hydrolyze the sole carbon source at the start of the fermentation, sucrose, into glucose and fructose, which the different microbial drivers use and induce many biochemical changes. Despite alcoholic fermentation by yeasts, ethanol levels remained relatively low during fermentation, suggesting that almost immediate oxidation of ethanol, by AAB, into acetic acid occurred. We actually observed a rapid increase in both yeast and AAB populations during the first 11 days which would be concomitant with these findings. In fact, AAB highly abundant in biofilm samples at the liquid-air interface thus ideal conditions would be encountered for efficient acetic acid production. Other organic acids also increased during fermentation (lactic, gluconic, glucuronic acids), remained at relatively stable levels (i.e. oxalic and succinic acids) or were only detected at low levels (malic acid). Some studies (Jia et al., 2016; Ku et al., 2010) have already shown that malic acid is present in *Camellia sinensis* (L.) O. Kuntze tea which is coherent with our results. Interestingly, malic acid could be transformed by the malolactic transformation by *O. oeni* (Wojdyło, Samoticha, & Chmielewska, 2020), thus leading to an increase of lactic acid as observed in our study. However, although a significant decrease of malic acid was observed between d0 and d7, it then increased during fermentation. Lactic acid can also be oxidized by AAB species into acetic acid and acetoin as observed in the present study (Moens et al., 2014). Among organic acids, highest concentrations were for acetic acid with levels reaching between 1.3 and 2.4 g/L, as frequently observed during Kombucha fermentations (Cardoso et al., 2020; Chakravorty et al., 2016; Coton et al., 2017). Lactic acid was the second most abundant acid with concentrations ranging between 0.3 and 0.8 g/L and most likely results from LAB fermentations. Among the other organic acids, glucuronic acid is considered as one of most important organic acids in Kombucha in regard to its potentially beneficial health properties. Indeed, this acid, by the glucuronidation process, has a detoxifying effect in humans by increasing the elimination of xenobiotics as well as endogenous metabolites as bilirubin, oxidized fatty acids and excess steroid hormones (Viña, Semjonovs, Linde, & Deniņa, 2014). It also increases transport and bioavailability of polyphenols, which are naturally present in the tea used for Kombucha fermentation, and can therefore increase the antioxidant properties of the beverage (Leal, Suárez, Jayabalan, Huerta, & Escalante-Aburto, 2018). Interestingly, this organic acid could be involved in the biosynthesis of other bioactive compounds as vitamin C or D-saccharic acid-1,4-lactone (Leal et al., 2018). Glucuronic acid production was described in AAB and interestingly (Nguyen, Dong, Nguyen, & Le, 2015) highlighted that symbiosis between *D. bruxellensis* and *Gluconacetobacter intermedius* strains leads to a higher production rate. Gluconic acid is also produced by AAB as

G. oxydans (Sainz et al., 2016) by oxidizing glucose. It was shown to be produced by some *Acetobacter* species when ethanol is depleted which is well correlated with our results as gluconic acid increased from d11 onwards. This organic acid is also of interest in Kombucha, but for its organoleptic properties. Indeed, this acid is naturally found in food products including fruits, plants, wine and honey and provides a refreshing sour taste (Sainz et al., 2016). Moreover, it is also used as an acidity regulator (E574) (Règlement (UE) N°1129/2011, n.d.) and has a pKa of 3.86, so in Kombucha, it probably leads to an acidity balance with acetic acid that has a pKa of 4.8.

Correlation analyses highlighted how the observed microbial shifts could be linked to certain changes in the volatilome profile. All species included in the tailor-made consortium were identified by metabarcoding. Two bacterial species, *A. okinawensis* and *L. nagelii*, dominated during fermentation and were well correlated to the mid or final fermentation stages, respectively, while among yeasts, *H. uvarum* dominated during the early fermentation stages before a clear shift was observed with *D. bruxellensis* dominating for the remainder of the fermentation. All four species also showed the strongest correlations with the identified volatile compounds. Interestingly, distinct changes in volatilome were directly linked to fermentation time with aldehydes and branched-chain alcohols most abundant in the first two fermentation stages (i.e. 3-methylbutanal associated with malty odors at day 7 and methylbutan-1-ol associated with waxy or soapy odors at days 11–14) followed by a much more complex volatilome profile between d20 and d27. During this final fermentation phase ethyl esters (i.e. sweet, fruity odors), acids (i.e. acidic, dairy or cheesy odors) and ketones (i.e. fruity or buttery odors) dominated and were well correlated with *D. bruxellensis*, *A. tropicalis* and *L. nagelii*. They may all contribute according to their detection thresholds, together with organic acids, to the overall sensorial properties of the final product. Noteworthy, fermentations using the tailor-made consortium were afterward conducted in a 1.5 L volume containers for sensory evaluation by comparing it to classically back-slop produced kombucha (using a 6-person panel). The performed hedonic tests, using a dedicated sensory evaluation table (overall acidity, acetic taste, sweetness, tannins and overall appreciation), confirmed a satisfactory product with acidic, citrus and slightly fruity odors and taste when compared to the control fermentation (data not shown). Like with other fermented beverages, the perception of some aroma compounds can be masked by the presence of others or enhanced due to synergistic effects. Among all the volatile compounds detected, acids and esters are most likely to shape the overall organoleptic property of the final product as directly linked to the most common and distinct descriptors of this product (i.e. acidic, refreshing, fruity...).

This study provides new insights on a tailor-made complex consortium to drive Kombucha fermentation and has provided a better understanding of the roles of each microbial species. The microbial drivers efficiently recreated a biofilm during fermentation which can be a useful alternative to the classical back-slopping procedure used for spontaneous fermentations. In the future, pilot or industrial scale fermentations using this tailor-made complex consortium should be done to confirm our results and further characterize the sensory properties and quality of the final product. It would also be necessary to confirm that these microbial drivers can avoid sluggish or slow fermentations in large-scale productions thus ensuring consumer satisfaction year-round. Also, different tailor-made consortia (i.e. simple versus complex) could be used to drive this fermentation and improve not only the sensorial properties but also potentially increase the beneficial health effects by increasing the production of certain key metabolites. Finally, the long-term goal would be to completely replace the classical SCOBY biofilm used as a starter and drive this fermentation with the tailor-made complex consortium.

Declaration of Competing Interest

The authors declare that they have no known competing financial

interests or personal relationships that could have appeared to influence the work reported in this paper.

Acknowledgments

We would like to thank Mr. Philippe Elies of the PIMMS platform at the UBO for the microscopy acquisitions.

Author contributions

MC, JM and EC obtained the funding and supervised the study. MC, JM and EC designed the experiments. OS performed experimental work and analysed the data. EP provided technical assistance for LC-MS analyses while JJ performed enzymatic organic acid determinations. AT and MM performed GC-MS analyses on tea samples. Metabarcoding analyses were done by JM. CD, OS, JJ, JM, EC and MC participated to sensorial analyses. Statistical and correlation analyses on all data were done by MC, MP and AT. OS and MC drafted the manuscript and all co-authors edited and proofread the manuscript.

Funding

This work was supported by the “Conseil régional de Bretagne” and CBB Capbiotek in the framework of the KombuchUP project (grant n°17001790). This research was carried out in collaboration with Biogroupe, France.

Appendix A. Supplementary material

Supplementary data to this article can be found online at <https://doi.org/10.1016/j.foodres.2021.110549>.

References

- Alexandre, H. (2013). Flor yeasts of *Saccharomyces cerevisiae*—their ecology, genetics and metabolism. *International Journal of Food Microbiology*, 167(2), 269–275. <https://doi.org/10.1016/j.ijfoodmicro.2013.08.021>.
- Arikan, M., Mitchell, A. L., Finn, R. D., & Gürel, F. (2020). Microbial composition of Kombucha determined using amplicon sequencing and shotgun metagenomics. *Journal of Food Science*, 85(2), 455–464. <https://doi.org/10.1111/1750-3841.14992>.
- Bechtner, J., Xu, D., Behr, J., Ludwig, C., & Vogel, R. F. (2019). Proteomic analysis of *Lactobacillus nagelii* in the presence of *Saccharomyces cerevisiae* isolated from water kefir and comparison With *Lactobacillus hordei*. *Frontiers in Microbiology*, 10, 325. <https://doi.org/10.3389/fmicb.2019.00325>.
- Bokulich, N. A., Collins, T. S., Masarweh, C., Allen, G., Heymann, H., Ebeler, S. E., & Mills, D. A. (2016). Associations among wine grape microbiome, metabolome, and fermentation behavior suggest microbial contribution to regional wine characteristics. *mBio*, 7, e00631–16. <https://doi.org/10.1128/mBio.00631-16>.
- Bourdichon, F., Casaregola, S., Farrokh, C., Frisvad, J. C., Gerd, M. L., Hammes, W. P., ... Hansen, E. B. (2012). Food fermentations: Microorganisms with technological beneficial use. *International Journal of Food Microbiology*, 154(3), 87–97. <https://doi.org/10.1016/j.ijfoodmicro.2011.12.030>.
- Callahan, B. J., McMurdie, P. J., Rosen, M. J., Han, A. W., Johnson, A. J. A., & Holmes, S. P. (2016). DADA2: High-resolution sample inference from Illumina amplicon data. *Nature Methods*, 13(7), 581–583. <https://doi.org/10.1038/nmeth.3869>.
- Caporaso, J. G., Kuczynski, J., Stombaugh, J., Bittinger, K., Bushman, F. D., Costello, E. K., ... Knight, R. (2010). QIIME allows analysis of high-throughput community sequencing data. *Nature Methods*, 7(5), 335–336. <https://doi.org/10.1038/nmeth.f.303>.
- Cardoso, R. R., Neto, R. O., dos Santos D'Almeida, C. T., do Nascimento, T. P., Presseste, C. G., Azevedo, L., ... de Barros, F. A. R. (2020). Kombuchas from green and black teas have different phenolic profile, which impacts their antioxidant capacities, antibacterial and antiproliferative activities. *Food Research International*, 128, 108782. <https://doi.org/10.1016/j.foodres.2019.108782>.
- Chakravorty, S., Bhattacharya, S., Chatzinotas, A., Chakraborty, W., Bhattacharya, D., & Gachhui, R. (2016). Kombucha tea fermentation: Microbial and biochemical dynamics. *International Journal of Food Microbiology*, 220, 63–72. <https://doi.org/10.1016/j.ijfoodmicro.2015.12.015>.
- Chen, C., & Liu, B. Y. (2000). Changes in major components of tea fungus metabolites during prolonged fermentation. *Journal of Applied Microbiology*, 89(5), 834–839. <https://doi.org/10.1046/j.1365-2672.2000.01188.x>.
- Costerton, J. W., Lewandowski, Z., Caldwell, D. E., Korber, D. R., & Lappin-Scott, H. M. (1995). Microbial biofilms. *Annual Review of Microbiology*, 49, 711–745. <https://doi.org/10.1146/annurev.mi.49.100195.003431>.
- Coton, M., Pawtowski, A., Taminiau, B., Burgaud, G., Deniel, F., Coulloumme-Labarthe, L., ... Coton, E. (2017). Unraveling microbial ecology of industrial-scale Kombucha fermentations by metabarcoding and culture-based methods. *FEMS Microbiology Ecology*, 93(5). <https://doi.org/10.1093/femsec/fix048>.
- De Filippis, F., Troise, A. D., Vitaglione, P., & Ercolini, D. (2018). Different temperatures select distinctive acetic acid bacteria species and promotes organic acids production during Kombucha tea fermentation. *Food Microbiology*, 73, 11–16. <https://doi.org/10.1016/j.fm.2018.01.008>.
- Dima, S.-O., Panaitescu, D.-M., Orban, C., Ghiurea, M., Doncea, S.-M., Fierascu, R. C., ... Oancea, F. (2017). Bacterial Nanocellulose from side-streams of Kombucha beverages production: Preparation and physical-chemical properties. *Polymers*, 9(8). <https://doi.org/10.3390/polym9080374>.
- Edgar, R. C., Haas, B. J., Clemente, J. C., Quince, C., & Knight, R. (2011). UCHIME improves sensitivity and speed of chimera detection. *Bioinformatics*, 27(16), 2194–2200. <https://doi.org/10.1093/bioinformatics/btr381>.
- Edwards, C. G., Collins, M. D., Lawson, P. A., & Rodriguez, A. V. (2000). *Lactobacillus nagelii* sp. nov., an organism isolated from a partially fermented wine. *International Journal of Systematic and Evolutionary Microbiology*, 50(2), 699–702. <https://doi.org/10.1099/00207713-50-2-699>.
- El-Taher, E. M. (2011). Kombucha: A new microbial phenomenon and industrial benefits. *African Journal of Biological Sciences*.
- Fremaux, B., Deniel, F., Mounier, J., Joubrel, R., Robieu, E., Pawtowski, A., ... Coton, M. (submitted). Microbial ecology of French dry fermented sausages and mycotoxin risk.
- Furukawa, S., Yoshida, K., Ogihara, H., Yamasaki, M., & Morinaga, Y. (2010). Mixed-species biofilm formation by direct cell-cell contact between brewing yeasts and lactic acid bacteria. *Bioscience, Biotechnology, and Biochemistry*, 74(11), 2316–2319. <https://doi.org/10.1271/bbb.100350>.
- Gaggia, F., Baffoni, L., Galiano, M., Nielsen, D. S., Jakobsen, R. R., Castro-Mejía, J. L., ... Di Gioia, D. (2019). Kombucha beverage from green, black and rooibos teas: A comparative study looking at microbiology, chemistry and antioxidant activity. *Nutrients*, 11(1), 1. <https://doi.org/10.3390/nu11010001>.
- Gomes, R., Borges, M., Rosa, M., Castro-Gómez, R., & Spínosa, W. (2018). Acetic Acid Bacteria in the Food Industry: Systematics, Characteristics and Applications. *Food Technology and Biotechnology*, 56. <https://doi.org/10.17113/ftb.56.02.18.5593>.
- Greenwalt, C. J., Steinkraus, K. H., & Ledford, R. A. (2000). Kombucha, the fermented tea: Microbiology, composition, and claimed health effects. *Journal of Food Protection*, 63(7), 976–981. <https://doi.org/10.4315/0362-028x-63.7.976>.
- Gromovych, T. I., Pigaleva, M. A., Gallyamov, M. O., Ivanenko, I. P., Ozerova, K. E., Kharitonova, E. P., ... Kiselyova, O. I. (2020). Structural organization of bacterial cellulose: The origin of anisotropy and layered structures. *Carbohydrate Polymers*, 237, 116140. <https://doi.org/10.1016/j.carbpol.2020.116140>.
- Haas, B. J., Gevers, D., Earl, A. M., Feldgarden, M., Ward, D. V., Giannoukos, G., ... Birren, B. W. (2011). Chimeric 16S rRNA sequence formation and detection in Sanger and 454-pyrosequenced PCR amplicons. *Genome Research*, 21(3), 494–504. <https://doi.org/10.1101/gr.112730.110>.
- Hall-Stoodley, L., Costerton, J. W., & Stoodley, P. (2004). Bacterial biofilms: From the natural environment to infectious diseases. *Nature Reviews Microbiology*, 2(2), 95–108. <https://doi.org/10.1038/nrmicro821>.
- Hesseltine, C. W. (1965). A millenium of fungi, food and fermentation. *Mycologia*, 57, 149–197.
- Hodel, K. V. S., Fonseca, L. M. dos S., Santos, I. M. da S., Cerqueira, J. C., dos Santos-Júnior, R. E., ... Machado, B. A. S. (2020). Evaluation of Different Methods for Cultivating *Gluconacetobacter hansenii* for Bacterial Cellulose and Montmorillonite Biocomposite Production: Wound-Dressing Applications. *Polymers*, 12(2). <https://doi.org/10.3390/polym12020267>.
- Ibáñez, A. B., & Bauer, S. (2014). Analytical method for the determination of organic acids in dilute acid pretreated biomass hydrolysate by liquid chromatography-time-of-flight mass spectrometry. *Biotechnology for Biofuels*, 7(1), 145. <https://doi.org/10.1186/s13068-014-0145-3>.
- Jankovic, I., & Stojanovic, M. (Faculty of A. (1994). Microbial and chemical composition, growth, therapeutical and antimicrobial characteristics of tea fungus. *Mikrobiologija (Yugoslavia)*. <https://agris.fao.org/agris-search/search.do?recordID=UY9600488>.
- Jayabalan, R., Malbaša, R. V., Lončar, E. S., Vitas, J. S., & Sathishkumar, M. (2014). A Review on Kombucha tea-microbiology, composition, fermentation, beneficial effects, toxicity, and tea fungus. *Comprehensive Reviews in Food Science and Food Safety*, 13(4), 538–550. <https://doi.org/10.1111/1541-4337.12073>.
- Jayabalan, R., Malini, K., Sathishkumar, M., Swaminathan, K., & Yun, S.-E. (2010). Biochemical characteristics of tea fungus produced during kombucha fermentation. *Food Science and Biotechnology*, 19(3), 843–847. <https://doi.org/10.1007/s10068-010-0119-6>.
- Jia, S., Wang, Y., Hu, J., Ding, Z., Liang, Q., Zhang, Y., & Wang, H. (2016). Mineral and metabolic profiles in tea leaves and flowers during flower development. *Plant Physiology and Biochemistry: PPB*, 106, 316–326. <https://doi.org/10.1016/j.plaphy.2016.06.013>.
- Kawarai, T., Furukawa, S., Ogihara, H., & Yamasaki, M. (2007). Mixed-species biofilm formation by lactic acid bacteria and rice wine yeasts. *Applied and Environmental Microbiology*, 73(14), 4673–4676. <https://doi.org/10.1128/AEM.02891-06>.
- Klindworth, A., Pruesse, E., Schweer, T., Peplies, J., Quast, C., Horn, M., & Glöckner, F. O. (2013). Evaluation of general 16S ribosomal RNA gene PCR primers for classical and next-generation sequencing-based diversity studies. *Nucleic Acids Research*, 41(1), Article e1. <https://doi.org/10.1093/nar/gks808>.
- Kolter, R., & Greenberg, E. P. (2006). The superficial life of microbes. *Nature*, 441(7091), 300–302. <https://doi.org/10.1038/441300a>.
- Ku, K. M., Choi, J. N., Kim, J., Kim, J. K., Yoo, L. G., Lee, S. J., ... Lee, C. H. (2010). Metabolomics analysis reveals the compositional differences of shade grown tea

- (*Camellia sinensis* L.). *Journal of Agricultural and Food Chemistry*, 58(1), 418–426. <https://doi.org/10.1021/jf902929h>.
- Kurtzman, C. P., Robnett, C. J., & Basehoar-Powers, E. (2001). Zygosaccharomyces kombuchaensis, a new ascosporegenous yeast from “Kombucha tea”. *FEMS Yeast Research*, 1(2), 133–138. <https://doi.org/10.1111/j.1567-1364.2001.tb00024.x>.
- Landis, E. A., Oliverio, A. M., McKenney, E. A., Nichols, L. M., Kfoury, N., Biango-Daniels, M., ... Wolfe, B. E. (2021). The diversity and function of sourdough starter microbiomes. *Elife*, 10, Article e61644. <https://doi.org/10.7554/eLife.61644>.
- Lê, S., Josse, J., & Husson, F. (2008). FactoMineR: An R package for multivariate analysis. *Journal of Statistical Software*, 25. <https://doi.org/10.18637/jss.v025.i01>.
- Leal, J., Suárez, L., Jayabalan, R., Huerta, J., & Escalante-Aburto, A. (2018). A review on health benefits of kombucha nutritional compounds and metabolites. *CyTA - Journal of Food*, 16, 390–399. <https://doi.org/10.1080/19476337.2017.1410499>.
- Lebleux, M., Abdo, H., Coelho, C., Basmaciyan, L., Albertin, W., Maupeu, J., ... Rousseaux, S. (2020). New advances on the *Brettanomyces bruxellensis* biofilm mode of life. *International Journal of Food Microbiology*, 318, 108464. <https://doi.org/10.1016/j.ijfoodmicro.2019.108464>.
- León-Romero, Á., Domínguez-Manzano, J., Garrido-Fernández, A., Arroyo-López, F. N., & Jiménez-Díaz, R. (2016). Formation of in vitro mixed-species biofilms by *Lactobacillus pentosus* and yeasts isolated from spanish-style green table olive fermentations. *Applied and Environmental Microbiology*, 82(2), 689–695. <https://doi.org/10.1128/AEM.02727-15>.
- Liu, C., Hsu, W., Lee, F., & Liao, C. (1996). The isolation and identification of microbes from a fermented tea beverage, Haipao, and their interactions during Haipao fermentation. *Food Microbiology*, 13(6), 407–415. <https://doi.org/10.1006/fmic.1996.0047>.
- Liu, D., Zhang, P., Chen, D., & Howell, K. (2019). From the vineyard to the winery: How microbial ecology drives regional distinctiveness of wine. *Frontiers in Microbiology*, 10, 2679. <https://doi.org/10.3389/fmicb.2019.02679>.
- Manz, W., Amann, R., Ludwig, W., Wagner, M., & Schleifer, K.-H. (1992). Phylogenetic oligodeoxynucleotide probes for the major subclasses of proteobacteria: Problems and solutions. *Systematic and Applied Microbiology*, 15(4), 593–600. [https://doi.org/10.1016/S0723-2020\(11\)80121-9](https://doi.org/10.1016/S0723-2020(11)80121-9).
- Markov, S. L., Malbasa, R. V., Hauk, M. J., & Cvetkovic, D. D. (University of N. S. (2001). Investigation of tea fungus microbe associations, 1: the yeasts. *Acta Periodica Technologica (Yugoslavia)*. <https://agris.fao.org/agris-search/search.do?recordID=UY2002000309>.
- Markov, S. L., Jerinić, V. M., Cvetković, D. D., Lončar, E. S., & Malbasa, R. V. (2003). *Kombucha - functional beverage: Composition, characteristics and process of biotransformation*. *Hemijiska Industrija*, 57(10), 456–462.
- Marsh, A. J., O'Sullivan, O., Hill, C., Ross, R. P., & Cotter, P. D. (2014). Sequence-based analysis of the bacterial and fungal compositions of multiple kombucha (tea fungus) samples. *Food Microbiology*, 38, 171–178. <https://doi.org/10.1016/j.fm.2013.09.003>.
- May, A., Narayanan, S., Alcock, J., Varsani, A., Maley, C., & Aktipis, A. (2019). Kombucha: A novel model system for cooperation and conflict in a complex multi-species microbial ecosystem. *PeerJ*, 7, e7565. <https://doi.org/10.7717/peerj.7565>.
- Mayer, P., Fromme, S., Leitzmann, C., & Grönder, K. (1995). The yeast spectrum of the “tea fungus Kombucha”. *Mycoses*, 38(7–8), 289–295. <https://doi.org/10.1111/j.1439-0507.1995.tb00410.x>.
- McDonald, D., Price, M. N., Goodrich, J., Nawrocki, E. P., DeSantis, T. Z., Probst, A., ... Hugenholtz, P. (2012). An improved Greengenes taxonomy with explicit ranks for ecological and evolutionary analyses of bacteria and archaea. *The ISME Journal*, 6(3), 610–618. <https://doi.org/10.1038/ismej.2011.139>.
- Mikkelsen, D., Flanagan, B. M., Dykes, G. A., & Gidley, M. J. (2009). Influence of different carbon sources on bacterial cellulose production by *Gluconacetobacter xylinus* strain ATCC 53524. *Journal of Applied Microbiology*, 107(2), 576–583. <https://doi.org/10.1111/j.1365-2672.2009.04226.x>.
- Moens, F., Lefeber, T., & De Vuyst, L. (2014). Oxidation of metabolites highlights the microbial interactions and role of *Acetobacter pasteurianus* during cocoa bean fermentation. *Applied and Environmental Microbiology*, 80(6), 1848–1857. <https://doi.org/10.1128/AEM.03344-13>.
- Montel, M.-C., Buchin, S., Mallet, A., Delbes-Paus, C., Vuitton, D. A., Desmasures, N., & Berthier, F. (2014). Traditional cheeses: Rich and diverse microbiota with associated benefits. *International Journal of Food Microbiology*, 177, 136–154. <https://doi.org/10.1016/j.ijfoodmicro.2014.02.019>.
- Mounier, J., Gelsomino, R., Goerges, S., Vancanneyt, M., Vandemeulebroecke, K., Hoste, B., ... Cogan, T. M. (2005). Surface microflora of four smear-ripened cheeses. *Applied and Environmental Microbiology*, 71(11), 6489–6500. <https://doi.org/10.1128/AEM.71.11.6489-6500.2005>.
- Nguyen, N. K., Dong, N. T. N., Nguyen, H. T., & Le, P. H. (2015). Lactic acid bacteria: Promising supplements for enhancing the biological activities of kombucha. *SpringerPlus*, 4, 91. <https://doi.org/10.1186/s40064-015-0872-3>.
- O'Donnell, K. (1993). *Fusarium and its near relatives*. In D. R. Reynolds and J. W. Taylor (ed.), *The fungal holomorph: mitotic, meiotic and pleomorphic speciation in fungal systematics*. CAB International (pp. 225–233).
- Penland, M., Deutsch, S.-M., Falentin, H., Pawtowski, A., Poirier, E., Visenti, G., ... Coton, M. (2020). Deciphering microbial community dynamics and biochemical changes during Nyons black olive natural fermentations. *Frontiers in Microbiology*, 11, 586614. <https://doi.org/10.3389/fmicb.2020.586614>.
- Podolich, O., Zaets, I., Kukhareno, O., Orlovska, I., Reva, O., Khirunen, L., ... Kozyrovska, N. (2017). The first space-related study of a Kombucha multimicrobial cellulose-forming community: Preparatory laboratory experiments. *Origins of Life and Evolution of the Biosphere: The Journal of the International Society for the Study of the Origin of Life*, 47(2), 169–185. <https://doi.org/10.1007/s11084-016-9483-4>.
- Pogačić, T., Maillard, M.-B., Leclerc, A., Hervé, C., Chuat, V., Yee, A. L., ... Thierry, A. (2015). A methodological approach to screen diverse cheese-related bacteria for their ability to produce aroma compounds. *Food Microbiology*, 46, 145–153. <https://doi.org/10.1016/j.fm.2014.07.018>.
- R Core Team. (2019). R: A language and environment for statistical computing. R Foundation for Statistical Computing. <https://www.r-project.org/>.
- Ramachandran, S., Fontanille, P., Pandey, A., & Larroche, C. (2006). *Gluconic acid: Properties, applications and microbial production* (p. 44). *Food Technology and Biotechnology*.
- Règlement (UE) N° 1129/2011. (n.d.). RÈGLEMENT (UE) N° 1129/2011 DE LA COMMISSION du 11 novembre 2011 modifiant l'annexe II du règlement (CE) N° 1333/2008 du Parlement européen et du Conseil en vue d'y inclure une liste de l'Union des additifs alimentaires.
- Reva, O. N., Zaets, I. E., Ovcharenko, L. P., Kukhareno, O. E., Shpylova, S. P., Podolich, O. V., ... Kozyrovska, N. O. (2015). Metabarcoding of the kombucha microbial community grown in different microenvironments. *AMB Express*, 5(1), 35. <https://doi.org/10.1186/s13568-015-0124-5>.
- Roller, C., Wagner, M., Amann, R., Ludwig, W., & Schleifer, K. H. (1994). In situ probing of gram-positive bacteria with high DNA G + C content using 23S rRNA-targeted oligonucleotides. *Microbiology (Reading, England)*, 140(Pt 10), 2849–2858. <https://doi.org/10.1099/00221287-140-10-2849>.
- Sainz, F., Jesús Torija, M., Matsutani, M., Kataoka, N., Yakushi, T., Matsushita, K., & Mas, A. (2016). Determination of dehydrogenase activities involved in D-glucose oxidation in *Gluconobacter* and *Acetobacter* strains. *Frontiers in Microbiology*, 7. <https://doi.org/10.3389/fmicb.2016.01358>.
- Spitaels, F., Wieme, A. D., Janssens, M., Aerts, M., Van Landschoot, A., De Vuyst, L., & Vandamme, P. (2015). The microbial diversity of an industrially produced lambic beer shares members of a traditionally produced one and reveals a core microbiota for lambic beer fermentation. *Food Microbiology*, 49, 23–32. <https://doi.org/10.1016/j.fm.2015.01.008>.
- Teoh, A. L., Heard, G., & Cox, J. (2004). Yeast ecology of Kombucha fermentation. *International Journal of Food Microbiology*, 95(2), 119–126. <https://doi.org/10.1016/j.ijfoodmicro.2003.12.020>.
- Tyakht, A., Kopeliovich, A., Klimenko, N., Efimova, D., Dovidchenko, N., Odintsova, V., ... Merkel, A. (2021). Characteristics of bacterial and yeast microbiomes in spontaneous and mixed-fermentation beer and cider. *Food Microbiology*, 94, Article 103658. <https://doi.org/10.1016/j.fm.2020.103658>.
- Villarreal-Soto, S. A., Beaufort, S., Bouajila, J., Souchard, J.-P., & Taillandier, P. (2018). Understanding Kombucha tea fermentation: A review. *Journal of Food Science*, 83(3), 580–588. <https://doi.org/10.1111/1750-3841.14068>.
- Villarreal-Soto, S. A., Bouajila, J., Pace, M., Leech, J., Cotter, P. D., Souchard, J.-P., ... Beaufort, S. (2020). Metabolome-microbiome signatures in the fermented beverage, Kombucha. *International Journal of Food Microbiology*, 333, 108778. <https://doi.org/10.1016/j.ijfoodmicro.2020.108778>.
- Vina, I., Semjonovs, P., Linde, R., & Denija, I. (2014). Current evidence on physiological activity and expected health effects of kombucha fermented beverage. *Journal of Medicinal Food*. <https://doi.org/10.1089/jmf.2013.0031>.
- Wang, Q., Garrity, G. M., Tiedje, J. M., & Cole, J. R. (2007). Naïve Bayesian classifier for rapid assignment of rRNA sequences into the new bacterial taxonomy. *Applied and Environmental Microbiology*, 73(16), 5261–5267. <https://doi.org/10.1128/AEM.00062-07>.
- Wang, S., Zhang, L., Qi, L., Liang, H., Lin, X., Li, S., ... Ji, C. (2020). Effect of synthetic microbial community on nutraceutical and sensory qualities of kombucha. *International Journal of Food Science & Technology*, 55. <https://doi.org/10.1111/ijfs.14596>.
- Wickham, H. (2016). *ggplot2: Elegant Graphics for Data Analysis* (2nd ed.). Springer International Publishing. <https://doi.org/10.1007/978-3-319-24277-4>.
- Wojdylo, A., Samoticha, J., & Chmielewska, J. (2020). The influence of different strains of *Oenococcus oeni* malolactic bacteria on profile of organic acids and phenolic compounds of red wine cultivars Rondo and Regent growing in a cold region. *Journal of Food Science*, 85(4), 1070–1081. <https://doi.org/10.1111/1750-3841.15061>.
- Yamada, Y., Yukphan, P., Lan Vu, H. T., Muramatsu, Y., Ochaikul, D., Tanasupawat, S., & Nakagawa, Y. (2012). Description of *Komagataeibacter* gen. nov., with proposals of new combinations (*Acetobacteraceae*). *The Journal of General and Applied Microbiology*, 58(5), 397–404. <https://doi.org/10.2323/jgam.58.397>.
- Yeluri Jonnala, B. R., McSweeney, P. L. H., Sheehan, J. J., & Cotter, P. D. (2018). Sequencing of the cheese microbiome and its relevance to industry. *Frontiers in Microbiology*, 9, 1020. <https://doi.org/10.3389/fmicb.2018.01020>.
- Zakrzewski, M., Proietti, C., Ellis, J. J., Hasan, S., Brion, M.-J., Berger, B., & Krause, L. (2017). Calypso: a user-friendly web-server for mining and visualizing microbiome-environment interactions. *Bioinformatics*, 33(5), 782–783. <https://doi.org/10.1093/bioinformatics/btw725>.
- Zhang, W., Wang, X., Qi, X., Ren, L., & Qiang, T. (2018). Isolation and identification of a bacterial cellulose synthesizing strain from kombucha in different conditions: *Gluconacetobacter xylinus* ZHCJ618. *Food Science and Biotechnology*, 27(3), 705–713. <https://doi.org/10.1007/s10068-018-0303-7>.